THE ASTROPHYSICAL JOURNAL, 457:625–644, 1996 February 1

UNCERTAINTIES IN THE MODELING OF OLD STELLAR POPULATIONS

STÉPHANE CHARLOT[1]
Kitt Peak National Observatory, 950 N. Cherry Avenue, Tucson, AZ 85726
GUY WORTHEY[2]
Department of Astronomy, University of Michigan, Ann Arbor, MI 48109-1090
AND
ALESSANDRO BRESSAN
Padua Astronomical Observatory, vicolo Osservatorio 5, 35122 Padova, Italy
Received 1995 May 26; accepted 1995 August 4

ABSTRACT

We compare three recent models of the spectral evolution of stellar populations to assess the origin of serious discrepancies in the colors predicted for $\gtrsim 1$ Gyr old populations of the same input age and metallicity. To isolate the source of these discrepancies, we investigate separately the two main characteristics of each model: the underlying stellar evolution prescription and the spectral calibrations used to transform the theoretical Hertzsprung-Russell diagram into observables. A 0.05 mag discrepancy in $B-V$ color is caused almost entirely by a known limitation of theoretical spectra. Differences in spectral calibrations are found to account for only a small fraction of the 0.25 mag discrepancies in $V-K$ color and of the 25% dispersion in mass-to–visual light ratio among the models considered here. The main source of disagreement for these quantities in the underlying stellar evolution prescription.

For idealized galaxies containing a single generation of stars and no dust, properties derived from broad-band colors using population synthesis models are found to be accurate by roughly $\pm 35\%$ in age at fixed metallicity, 25% in metallicity at fixed age if the heavy-element mixture is assumed to be scaled-solar, and 35% in mass at fixed metallicity and fixed initial mass function. These indicative uncertainties are based on the dispersion in the predictions of the models investigated here.

There appear to be persistent problems in virtually every ingredient of population synthesis models. The most serious are the lifetimes and luminosities of stars in post–main-sequence evolutionary stages; the temperature of the red giant branch and color-temperature relation for cool stars; and the lack of accurate libraries of stellar spectra, especially for cool stars and for nonsolar metallicities. These problems have profound causes. The main one is the high sensitivity of stellar evolution models on the efficiency of several critical factors which are either not sufficiently understood or cannot yet be determined uniquely from comparisons with observations (opacities, heavy-element mixture, helium content, convection, diffusion, mass loss, rotational mixing). Other major limitations are the difficult spectral modeling of cool stars and the unavailability of calibration stars for metal-rich populations and populations with altered chemical mixes.

Subject headings: galaxies: evolution — galaxies: photometry — galaxies: stellar content — stars: evolution

1. INTRODUCTION

The integrated light from star clusters and galaxies should reflect the distribution of initial mass functions (IMFs), ages, and metallicities within them, providing us with important clues on the past history of star formation. Stellar population synthesis, the modeling of the spectral energy distribution emitted by specific populations of stars, is a natural approach to identifying such clues. Studies in this field have led to the development of population synthesis models, usually termed "evolutionary" (Crampin & Hoyle 1961; Tinsley 1978; Bruzual 1983; Arimoto & Yoshii 1987; Guiderdoni & Rocca-Volmerange 1987; Buzzoni 1989; Bruzual & Charlot 1993, 1995; Bressan, Chiosi, & Fagotto 1994; Fritze von Alvensleben & Gehrard 1994; Worthey 1994; Mayya 1995; Weiss, Peletier, & Matteucci 1995). In such models the main adjustable parameters are usually the stellar IMF, the star formation rate, and in some cases the rate of chemical enrichment. For a given set of parameters one computes the time-dependent distribution of stars in the theoretical Hertzsprung-Russell diagram (hereafter H-R diagram), from which the integrated spectral evolution of the stellar population can be obtained. These models are widely used to study stellar systems which are too far away for individual stars to be discerned.

Despite decades of effort, the star formation and chemical evolution history of distant galaxies remains a mystery. Part of the problem is that spectral evolution is slow if the youngest stars present are older than about 1 Gyr (Tinsley 1972). Another problem is that both age and metallicity have a similar effect on integrated colors and line strengths. If two stellar populations differ in age and metallicity by $d\log \mathrm{age}/d\log Z \approx 3/2$, they will appear virtually identical in all colors and most optical spectral indices (Worthey 1994).

Unfortunately, these difficulties in recovering the mixture of stars in a galaxy from observations of the integrated light are further aggravated by significant differences among existing models in the predicted spectral properties of a stellar population with fixed age and metallicity. For example, the age inferred for an old, passively evolving galaxy with solar metallicity and optical/infrared colors $B-V \approx 0.9$ and $V-K \approx 3.3$ can range from roughly 4 to 13 Gyr, depending on the model

[1] On leave from the Institut d'Astrophysique du Centre National de la Recherche Scientifique, Paris, France.
[2] Hubble Fellow.

used (e.g., Figs. 34 and 35 of Worthey 1994). Such large discrepancies are bound to be caused by differences in the main underlying assumptions, which we conveniently divide into two categories: the stellar evolution theory used to predict the distribution of stars in the theoretical H-R diagram and the library of spectra assigned to stars as a function of temperature and luminosity, from which colors are calculated. The magnitude and color scales of most new models of stellar population synthesis have been tested satisfactorily against observations of star clusters (Buzzoni 1989; Bruzual & Charlot 1993; Bressan et al. 1994; Worthey 1994; Girardi et al. 1995). In spite of this, the models also lead to widely different interpretations of galaxy spectra.

Our purpose in this paper is to reevaluate the uncertainties in stellar population synthesis models by analyzing in detail, as an example, the origin of the discrepancies between three recent models (Bertelli et al. 1994; Worthey 1994; Bruzual & Charlot 1995). We hope to alert users of these models to problems both real and potential, and to roughly gauge the uncertainties in the results of evolutionary synthesis calculations. To warrant overlap between the different models, we investigate here only the properties of stellar populations older than about 1 Gyr. The uncertainties arising in the modeling of younger stellar populations are briefly addressed in § 5.7. In § 2 below, we review the characteristics of the models under consideration and point out some of the differences in the associated spectrophotometric predictions. We then elucidate in §§ 3 and 4 the parts of the discrepancies arising from, respectively, the different stellar evolution theories and different spectral calibrations adopted in the models. Finally, in § 5, we discuss the origin of persistent uncertainties in the various ingredients of modern population synthesis models and evaluate the reliability of using such models to interpret observations of star clusters and galaxies.

2. CHARACTERISTICS OF THREE RECENT MODELS

2.1. *General Description*

We first briefly recall the characteristics of three recent models used in the next sections to exemplify the uncertainties inherent in the modeling of stellar populations. The models of Bertelli et al. (1994, hereafter BBCFN), Worthey (1994, hereafter GW), and Bruzual & Charlot (1995, hereafter B&C) each include different updates in the theories of stellar interiors and atmospheres. These models are ideally suited for the present analysis because they all relate to a similar technique of "isochrone synthesis" to predict the spectral evolution of stellar populations (Charlot & Bruzual 1991). The technique is based on the property that stellar populations with any star formation history can be expanded in series of instantaneous bursts. Thus, the spectrophotometric properties of stellar populations with arbitrary star formation rates and chemical enrichment rates can be obtained by means of simple convolution integrals of isochrones for instantaneous burst populations with fixed IMFs and metallicities. In return, differences in the properties predicted for any stellar population can be traced back to differences in the isochrones predicted for instantaneous burst populations with fixed IMFs and metallicities. We now describe the main relevant features of the models above, referring the reader to the original papers for full details. These features are summarized in Table 1. The implications of our results for the predictions of other modern population synthesis models will be addressed in § 5.

The B&C stellar population synthesis models have solar metallicity and include all phases of stellar evolution from the zero-age main sequence to supernova explosion (for progenitors with mass $m > 8\ M_\odot$) or the end of the white-dwarf cooling sequence (for less massive progenitors). The 1995 models used here present a few corrections and updates with respect to the Bruzual & Charlot (1993) models. These revisions are mentioned in § 2.2, and their implications for the photometric predictions are illustrated in Figure 1. Two sets of stellar evolutionary tracks can be chosen in the new B&C models: one based on the computations by Schaller et al. (1992) (for $m > 2\ M_\odot$), Charbonnel et al. (1995) (for $0.8 \leq m \leq 2\ M_\odot$), and Bressan et al. (1993) (for $0.6 \leq m \leq 0.8\ M_\odot$), referred to as the Geneva set. The other tracks are based on the computations by Bressan et al. (1993), referred to as the Padua set. The two sets were supplemented with a semi-empirical prescription for the thermally pulsing regime at the end of the asymptotic giant branch (TP-AGB), with post-AGB evolutionary tracks, and with unevolving main-sequence stars in the mass range $0.1 \leq 130.6\ M_\odot$ (see also Charlot & Bruzual 1991). The Geneva tracks include mild overshooting in the convective cores of stars more massive than $1.5\ M_\odot$, as indicated by various observations of Galactic star clusters (see however § 5.3).[3] The abundances are $X = 0.68$, $Y = 0.30$, and $Z = 0.02$, and the opacities are from Rogers & Iglesias (1992) (for $m \geq 2\ M_\odot$), Iglesias & Rogers (1993) (for $2 > m \geq 0.8\ M_\odot$), and Iglesias, Rogers, & Wilson (1992) (for $0.8 > m \geq 0.6\ M_\odot$). The models are normalized to the luminosity, temperature, and radius of the Sun at an age of 4.6 Gyr. The characteristics of the Padua tracks are recalled below in the description of the BBCFN models.

Most of the stellar spectra in the B&C models were taken directly from observations of Galactic stars at near-ultraviolet, optical, and near-infrared wavelengths. The ultraviolet spectra are from the *International Ultraviolet Explorer* and *Orbiting Astronomical Observatory* databases. The optical spectra are from Gunn & Stryker (1983), and the near-infrared spectra from Persson (1987) and Fluks et al. (1994). The resulting spectral library encompasses the luminosity classes III, IV, V and all spectral types from O5 ($T_{\rm eff} \sim 40{,}000$ K) to M10 ($T_{\rm eff} \sim 2500$ K). The observed stellar spectra were extended into the far-ultraviolet using the Kurucz (1979) model atmospheres. The spectra of stars with effective temperatures in the range $40{,}000 < T_{\rm eff} \leq 50{,}000$ K were approximated at all wavelengths by the Kurucz models. The spectra of hotter stars were approximated by unblanketed blackbodies. The assignment of a spectrum to a star at any position in the H-R diagram was performed by first transforming the tracks from the log $T_{\rm eff}$-log L diagram to the (V, $B-V$) diagram using standard calibration relationships (Böhm-Vitense 1972; Flower 1977; Buser & Kurucz 1978). Then, a star was assigned the available spectrum with closest optical/infrared colors according to Johnson's (1966) calibration of the *UBVRIJKL* photometric system as a function of $B-V$ color and luminosity class. For giant stars cooler than about 5000 K, the Ridgway et al. (1980) $V-K$ color-temperature scale was used. Finally, the selected spectra were scaled in flux by computing the absolute V flux corresponding to the calibrated bolometric correction of the

[3] "Convective overshooting" refers to the increase of the convective zone when its boundary is defined where the velocities of convective elements vanish, instead of where their acceleration vanishes (the standard $\nabla T_{\rm rad} = \nabla T_{\rm ad}$ Schwarzschild criterion). The main effect of overshooting on stellar evolution is to increase the convective core size, and hence the main-sequence lifetime and luminosity (e.g., Maeder 1975; Bertelli, Bressan, & Chiosi 1985).

TABLE 1

CHARACTERISTICS OF THREE STELLAR POPULATION SYNTHESIS MODELS

Parameter	B&C	GW	BBCFN
Interior opacities	1992, 1993	1977	1992
Convective overshooting	Mild	None	Mild
Flux library	Empirical	Kurucz 1992[a]	Kurucz 1992[a]
M giants spectra	Gunn & Stryker 1983 Persson 1987 Fluks et al. 1994	Bessell et al. 1989[a] Gunn & Stryker 1983	Straizys & Sviderskiene 1972 Terndrup et al. 1991 Lançon & Rocca-Volmerange 1992
M giants temperatures	Ridgway et al. 1980	Ridgway et al. 1980	Ridgway et al. 1980 Lançon & Rocca-Volmerange 1992
$BC_{V\odot}$	−0.04	−0.12	−0.08
$M_{bol\odot}$	4.75	4.72	4.77
$(B-V)_{Vega}$	0.00	0.00	−0.003
$(V-K)_{Vega}$	0.00	0.01	0.00
Metallicity	$Z_\odot$	0.01 $Z_\odot$–3 $Z_\odot$	0.02 $Z_\odot$–5 $Z_\odot$
IMF range	0.1–120 $M_\odot$	0.1–2 $M_\odot$	0.15–120 $M_\odot$
Available ages	$t \geq 0$	$t \geq 1.5$ Gyr	$t \geq 0$

[a] Model atmospheres.

stars (Code et al. 1976). The spectra of TP-AGB stars were calibrated separately using the colors of Mira Ceti and IK Tau (see Charlot & Bruzual 1991).

The BBCFN stellar isochrones constitute the basis of the Bressan et al. (1994) population synthesis models and recent revisions and extensions by Bressan, Chiosi, & Tantalo (1995)

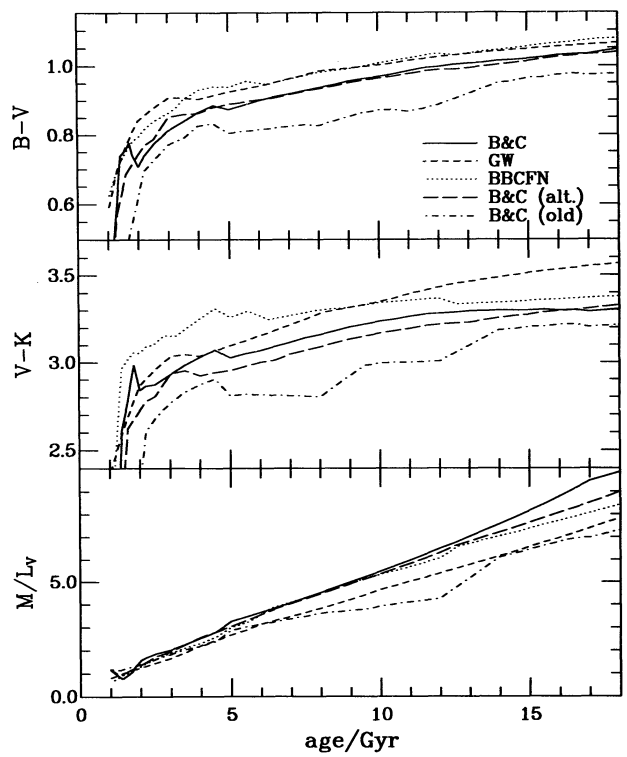

FIG. 1.—Evolution of the $B-V$ and $V-K$ colors and mass-to-visual light ratio M/L_V of an instantaneous-burst stellar population with solar metallicity according to several recent population synthesis models (Bruzual & Charlot 1995 using the Geneva [B&C] and Padua [B&C alt.] tracks; Bertelli et al. 1994 [BBCFN]; Worthey 1994 [GW]; Bruzual & Charlot 1993 [B&C old]). The models have the Salpeter IMF with lower an upper cutoffs $m_L = 0.15\ M_\odot$ and $m_U = 2\ M_\odot$, respectively. The passbands of tlie B and V filters are from Buser & Kurucz (1978) in the B&C and BBCFN models and from Bessell (1990) in the GW model. The passband of the K filter is from Bessell & Brett (1988) in the GW and BBCFN models, and from Palomar Observatory in the B&C model (provided by S. E. Persson).

and Tantalo et al. (1995). The isochrones rely on a comprehensive set of stellar evolutionary tracks by Alongi et al. (1993), Bressan et al. (1993), and Fagotto et al. (1994a, b, c) encompassing a wide range of initial chemical compositions, from $Z = 0.0004$ to $Z = 0.1$ with $Y = 2.5Z + 0.23$ ($Z_\odot = 0.02$ and $Y_\odot = 0.28$) assumed. The tracks were computed using the radiative opacities by Iglesias et al. (1992) and include all phases of stellar evolution from the zero-age main sequence to remnant stage for stars in all mass ranges. For solar composition, the models are normalized to the temperature, luminosity, and radius of the Sun at an age of 4.6 Gyr. The amount of overshooting in the convective cores of stars more massive than 1.5 $M_\odot$ is similar to that adopted by Schaller et al. (1992). Overshooting is also included, with a reduced efficiency, in the cores of stars with masses between 1.0 and 1.5 $M_\odot$. The tracks used by BBCFN further include efficient overshooting in the convective envelopes of low- and intermediate-mass stars, as appears to be suggested by detailed observations of the red giant branch (RGB) and horizontal branch of star clusters in the Galactic halo and the Large Magellanic Cloud (hereafter LMC; Alongi et al. 1991). BBCFN supplemented this homogeneous set of tracks with an analytic prescription for the thermally pulsing regime of low- and intermediate-mass stars at the end of the AGB and by post-AGB evolutionary tracks.

The inclusion of stars with nonsolar metallicities forced BBCFN to appeal to model atmospheres to make spectrophotometric predictions because too few stars of this kind have been observed so far (see also Bressan et al. 1994). The Kurucz (1992) model atmospheres were used to approximate the spectra of stars with temperatures in the range $3500 < T_{\rm eff} \leq 50{,}000$ K at all wavelengths. The spectra of hotter stars were approximated by unblanketed blackbodies. The spectra of cooler stars were constructed from a composite of three catalogs of observational spectra of Galactic disk and bulge stars (Straizys & Sviderskiene 1972; Terndrup, Frogel, & Whitford 1991; Lançon & Rocca-Volmerange 1992). Stars on the evolutionary tracks were then assigned spectra in a similar way as in B&C. The procedure is simpler in the case of model atmospheres because the effective temperature and bolometric correction associated to a given spectrum are known in advance. For cool giants, Bressan et al. (1994) first calibrated the observational spectra using a combination of the color-temperature scales of Ridgway et al. (1980) and Lançon & Rocca-Volmerange (1992). The BBCFN isochrones include a revision

of this prescription motivated by the matching of the observed *BVRI* color-magnitude diagram of the metal-rich globular cluster NGC 6553 (Ortolani, Barbuy, & Bica 1990).

GW also developed new stellar population synthesis models for a wide range of metallicities. His models are based on a core amalgamation of stellar evolutionary isochrones by VandenBerg and collaborators and the Revised Yale Isochrones (VandenBerg 1985; VandenBerg & Bell 1985; VandenBerg & Laskarides 1987; Green, Demarque, & King 1987). The stellar models underlying the isochrones were computed using the classical theory of convection (no overshooting), and the opacities are from the Los Alamos Astrophysical Opacity Library (Huebner et al. 1977). The isochrones extend from the middle main sequence to the tip of the RGB, and the various chemical compositions range from $Z = 0.0001$ to $Z = 0.1$ with $Y = 2.7Z + 0.228$ ($Z_\odot = 0.0169$ and $Y_\odot = 0.274$) assumed. The GW models, which have explicit Y-dependence, show that small changes in Y have small effects on the integrated properties of stellar populations (see, however, § 5.3 below). For solar abundances, the models are again normalized to the temperature and luminosity of the Sun at an age of 4.6 Gyr. GW extended these isochrones down the lower main sequence using stellar evolutionary tracks by VandenBerg (1983). The evolution beyond the tip of the RGB was approximated by a single red clump for the core-helium burning phase, and by isochrones inferred from various theoretical prescriptions through the early AGB up to the thermally pulsing regime at the end of the AGB. The final isochrones assembled in this way can be used to describe the properties of stellar populations with ages between 1.5 and 18 Gyr for most metallicities.

Since the GW models also include nonsolar metallicity stars, the spectra of stars hotter than 3750 K were again approximated by the Kurucz (1992) model atmospheres. For cooler stars, composite spectra were assembled by patching together model atmospheres (Bessell et al. 1991, and references therein) and optical observational spectra of M giants by Gunn & Stryker (1983). Blackbody tails were attached at the extreme ends of the spectra before computing colors and bolometric corrections. The temperature scale as a function of $V-K$ color for giant, solar-metallicity stars with temperatures in the range $3250 \lesssim T_{\rm eff} \lesssim 5000$ K was found to be in good agreement with the empirical calibration of Ridgway et al. (1980), except around $T_{\rm eff} \approx 3500$ K, where the models appear to be about 0.5 mag bluer. Furthermore, in warm giants (around 5000 K) the predicted $B-V$ color based on Kurucz model fluxes was found to be systematically redder by about 0.06 mag than the empirical prescriptions of Johnson (1966) (see also Peterson, Dalle Ore, & Kurucz 1993). GW did not attempt to correct for these defects.

The above description summarizes the differences in stellar evolution prescriptions and spectral calibrations among three recent population synthesis models. Figure 1 illustrates some of the resulting discrepancies in the photometric predictions of the models. The evolution of the $B-V$ and $V-K$ colors and of the mass-to-visual light ratio, M/L_V, are shown for an instantaneous burst stellar population with solar metallicity as computed alternatively with the B&C (using either the Geneva or Padua tracks), GW, and BBCFN models. The passbands adopted for the B, V, and K filters are listed in the caption. We have assumed that stars form with the Salpeter IMF $\phi(m) \propto m^{-2.35}$ (where $\phi[m]dm$ is proportional to the number of stars born with masses between m and $m + dm$). Furthermore, the common IMF adopted for all models in Figure 1 and in the remainder of this paper has lower and upper cutoffs $m_L = 0.15\ M_\odot$ and $m_U = 2\ M_\odot$, respectively. The lower mass cutoff is imposed by the BBCFN model and the higher mass cutoff by the GW model.

The predicted evolution of the $B-V$ color is similar in the GW and BBCFN models and is 0.04 to 0.07 mag bluer in the B&C model computed with either the Geneva or Padua tracks. The various models differ more markedly in the predicted evolution of the $V-K$ color. The GW model is systematically redder than the B&C model, the discrepancy increasing steadily from less than 0.2 mag at an age of 2 Gyr to nearly 0.3 mag at an age of 17 Gyr. In contrast, the difference in $V-K$ color between the BBCFN and GW models ranges from $+0.2$ mag at an age of 4 Gyr to -0.2 mag at an age of 17 Gyr. Also, substituting the Padua tracks for the Geneva tracks in the B&C model reduces the predicted $V-K$ color by about 0.1 mag at ages less than 15 Gyr. These deviations are large compared to typical observational uncertainties, and they imply alarming ambiguities in the interpretation of galaxy colors. Figure 1 also shows that the update of the Bruzual & Charlot (1993) model by B&C has resulted in a systematic reddening of the $B-V$ color by 0.05 to 0.1 mag at ages greater than 2 Gyr, and a reddening of the $V-K$ color by up to 0.3 mag at ages between 2 and 12 Gyr (see § 2.2 below). Finally, the bottom panel of Figure 1 indicates that the luminosity at fixed stellar population mass is similar in the B&C and BBCFN models, but systematically larger in the GW model. These combined discrepancies are to be unraveled in §§ 3 and 4.

It is worth noting that the large differences in the predictions of the various models in Figure 1 cannot be straightforwardly resolved by means of comparisons with observations. In fact, the models all compare to the observed colors of star clusters and early-type galaxies approximately in a similar way. This is shown in Figure 2, in which the $B-V$, $U-V$, and $V-K$ colors of the solar-metallicity models of Figure 1 are plotted for ages 1–18 Gyr against integrated colors for Galactic and M31 globular clusters (Burstein et al. 1984), LMC clusters older than about 1 Gyr (van den Bergh 1981; Persson et al. 1983), and elliptical and S0 galaxies (Frogel et al. 1978; Peletier 1989). The general agreement between model and observed color sequences is all the more remarkable in that the data, unlike the models, include a wide range of metallicities. Globular clusters have metallicities in the range $-2.2 \lesssim$ [Fe/H] $\lesssim -0.5$ and are presumably uniformly old (e.g., Hesser 1993). Elliptical and S0 galaxies probably contain several generations of stars (see also § 5.8 below), although they usually are not expected to have experienced large recent bursts of star formation. According to González (1993), the dominant stellar populations in these galaxies would have metallicities slightly less than twice solar. The younger LMC clusters in Figure 2 (with ages $\gtrsim 1$ Gyr) have [Fe/H] ≈ -0.25, but the older clusters are probably as metal-poor as Galactic globular clusters (e.g., Cohen 1982).

Figure 2 illustrates the lack of clear diagnostic diagrams in integrated broadband colors for population synthesis models. For example, while at fixed metallicity colors tend to redden with age (Fig. 1), the higher metallicity of the younger LMC clusters in Figure 2 causes their colors to be redder than those of the old, more metal-poor clusters. We note that the scatter in $V-K$ color for the younger LMC clusters is caused by the high sensitivity of the integrated light to the presence of even a few extremely cool carbon stars in these objects (carbon stars are not included in any of the models; see § 5.4 for more detail). Furthermore, the relatively blue colors in Figure 2 of one S0

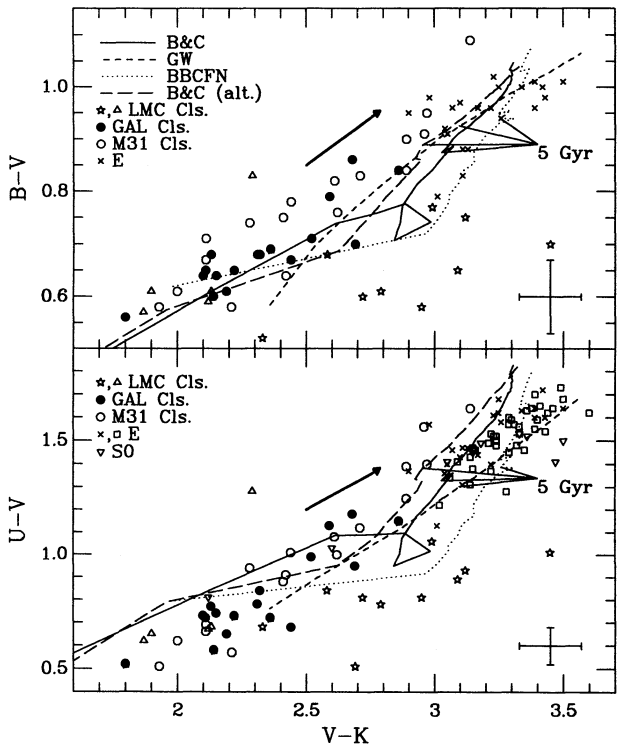

FIG. 2.—Comparison of the $B-V$, $U-V$, and $V-K$ colors predicted by the solar-metallicity models of Fig. 1 at ages 1–18 Gyr with observed colors for star clusters and galaxies (all corrected for reddening). Model loci at 5 Gyr are also marked. The loop drawn in both panels by the B&C model based on the Geneva tracks is caused by a drop in the AGB contribution to the integrated light around 1.5 Gyr, which also shows up as spikes in the upper two panels of Fig. 1. Colors for Galactic and M31 globular clusters come from Burstein et al. (1984). For LMC clusters *UBV* colors are from van den Bergh (1981) and $V-K$ colors are from Persson et al. (1983). The LMC clusters are divided into two categories: upright triangles refer to the oldest clusters (type VII in the Searle, Wilkinson, & Bagnuolo 1980 classification), which have similar characteristics as old, metal-poor Galactic globular clusters, and stars refer to younger clusters (types IV, V, and VI), which have ages in the range 1–15 Gyr and metallicities in the range $-2 \lesssim [Fe/H] \lesssim -0.25$ (increasing with decreasing age). The scatter of LMC clusters to red $V-K$ color is caused by the stochastic presence of carbon stars on the upper AGB (carbon star spectra are not included in any of the models). Aperture photometry of elliptical (*squares*) and S0 (*upside down triangles*) galaxies are from Frogel et al. (1978), and colors at the 5″ and outermost measured radii of 12 elliptical galaxies (*crosses*) are from the surface photometry of Peletier (1989). Conservative maximum observational error bars are indicated on the bottom right of each panel. Typical random errors are smaller, about 0.02 mag in $B-V$ and 0.05 mag in $U-V$ and $V-K$. Arrows representing the effect of reddening for $E(B-V) = 0.1$ mag indicate how extinction can further aggravate the age-metallicity degeneracy.

galaxy of nearly solar metallicity which recently underwent a burst of star formation (the local group galaxy NGC 205 with $V-K = 2.1$ and $U-V = 0.8$; e.g., Davidge 1992) coincide with the colors of the most metal-poor, oldest clusters in the Galaxy. This provides dramatic empirical evidence of the severity of the age-metalliciy degeneracy. The rough match by solar-metallicity models in Figure 2 to the color sequences of star clusters and early-type galaxies is another example of this degeneracy. Extinction can further aggravate the age-metallicity degeneracy, as reddening vectors are parallel to the age/metallicity color sequences in Figure 2. In the present study, we do not include the effects of dust on the photometric predictions of population synthesis models.

2.2. *Errata*

The main purpose of the present paper is to investigate legitimate differences in the predictions of population synthesis models. Unfortunately for potential users of such models, involuntary mistakes and progressive fine-tuning can also contribute to confusion. As a by-product of our comparison, we have found and corrected several mistakes in previously published versions of the models. These are listed here.

In Table 3 of GW, the final entry for the $V-K$ color from models corrected to the Johnson (1966) color tables should be 3.258, not 3.292. This error, which is due to a programming mistake, caused GW to have more confidence in the model $V-K$ color than is actually warranted.

In Bruzual & Charlot (1993), a label mismatch along the points of the isochrones implied that the numbers of stars calculated for one bin were shifted to the previous bin. A most noticeable effect of this mistake was that a large group of stars that should have been burning helium on the horizontal branch was instead put at the tip of the RGB, making the integrated colors redder. Similarly, the lower TP-AGB phase was included in the early-AGB phase, which modifies significantly the predicted relative contributions by early- and TP-AGB stars to the integrated light of star clusters in Figure 4*b* of Charlot & Bruzual (1991), although the total AGB contribution remains virtually unchanged. The reason why the revised B&C models predict colors even redder than the Bruzual & Charlot (1993) models is that they also include revisions of the evolutionary tracks for low-mass stars and of the bolometric corrections for cool stars. These various issues are discussed in greater detail by B&C.

In BBCFN, the values of the integrated $V-J$, $V-H$, and $V-K$ colors listed at the bottom of the original isochrone (PostScript) tables distributed by the authors are wrong because of a printing error. In addition, the assignment of cool star spectra as a function of effective temperature in BBCFN went beyond the published description, since the final color-$T_{\rm eff}$ relation was in reality tuned by the comparison with *BVRI* color-magnitude diagrams of a metal-rich globular cluster (see § 2.1 above). This ensures that color-magnitude diagrams are matched and may improve the accuracy of the integrated colors, but this also hides potential errors in the color-$T_{\rm eff}$ relation. Finally, in Bressan et al. (1994), the spectrum assigned to the first point on the horizontal branch was erroneously given a temperature midway between the true temperature and that on the tip of the RGB. This effect becomes noticeable at old ages and high metallicities making $V-K$ colors bluer by up to 0.6 mag for old, $Z = 0.05$ populations. The reader should refer to the new models of Tantalo et al. (1995), which supersede those of Bressan et al. (1994).

All the errors listed above were corrected before using the models for the purpose of the present paper. This implies that the model predictions shown here may not match previously published values (except for the Bruzual & Charlot 1993 predictions recalled in Fig. 1). The models used here also differ from those published elsewhere in the choice of the IMF, which has been truncated to a lower cutoff of 0.15 $M_\odot$ in the B&C and GW models and extended to this limit in the BBCFN model.

3. INFLUENCE OF THE STELLAR EVOLUTION PRESCRIPTIONS

In this section we estimate the amount of the discrepancy in the photometric predictions of the three models described in the previous section originating from differences in the stellar

evolution prescriptions. To achieve this, we extract the theoretical isochrones from the different models and adopt only one library of stellar spectra, that of B&C, to compute photometric properties. We begin by comparing the predicted effective temperature, luminosity, and mass of stars along the isochrones at the ages of 2 and 12 Gyr that correspond to different types of model mismatches in Figure 1. We then analyze the number distribution of stars as a function of evolutionary stage along these isochrones and the implied distributions of optical and infrared light in the three models (again, at fixed spectral calibrations). The reader interested only in the main conclusions of these comparisons is referred to the last two paragraphs of the section. Except as otherwise indicated, all predictions of the B&C model shown in the remainder of this paper are based on the Geneva tracks, the effect of switching to the Padua tracks option being already illustrated by the predictions of the BBCFN model.

Figure 3 shows the B&C, BBCFN, and GW theoretical isochrones for an instantaneous burst stellar population at an age of 2 Gyr. The isochrones at an age of 12 Gyr are shown in Figure 4. We do not show the extension of the BBCFN and B&C isochrones beyond the AGB phase because GW did not include post-AGB stars (the contribution to the integrated light by these stars is significant only at wavelengths blueward of $\sim$3000 Å; see § 5.5). The differences between the isochrones in Figures 3 and 4 can be better described by delineating discrepancies in stellar temperature, luminosity, and mass as a function of evolutionary phase. This is shown in Figures 5 and 6 for the isochrones at 2 and 12 Gyr, respectively. Here, we have resampled all isochrones to a common system of 150 evolutionary phases, in which phase 55 is the main-sequence turnoff, phase 100 the RGB tip, phase 120 the base of the early-AGB, phase 140 the base of the TP-AGB, and phase 150 the end of the TP-AGB (see, e.g., GW for details on the construction of a similar system).

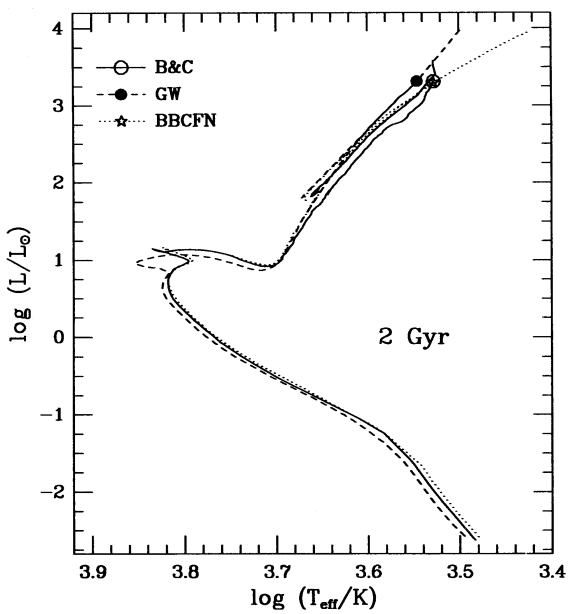

FIG. 3.—Theoretical isochrone of a 2 Gyr old, instantaneous-burst stellar population with solar metallicity according to the B&C, BBCFN, and GW models. Main-sequence stars less massive than 0.15 $M_\odot$ in the B&C and GW models and post-AGB stars in the B&C and BBCFN models have been removed for comparison purposes. The different symbols indicate the locus of the RGB tip in the three models.

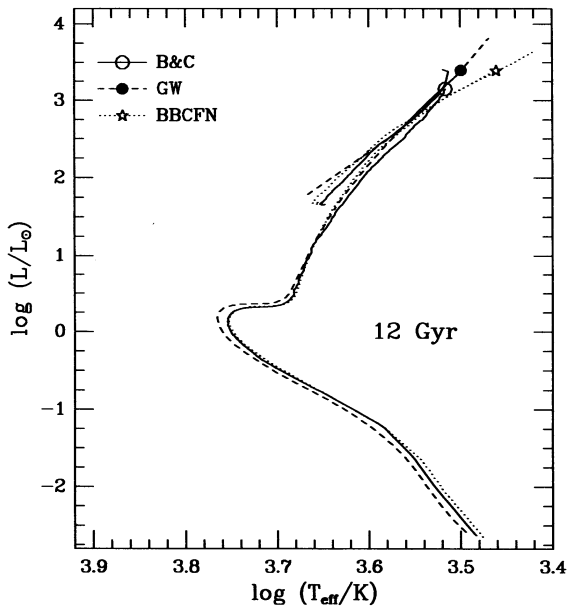

FIG. 4.—Same as Fig. 3, but for an age of 12 Gyr

Figures 3 to 6 reveal small but significant differences in the predicted isochrones. At 2 Gyr, the turnoff stars are significantly less massive and fainter in the GW model than in the B&C and BBCFN models, in which the inclusion of overshooting increases the lifetimes of stars more massive than 1–1.5 $M_\odot$. Turnoff and subgiant stars are also slightly warmer

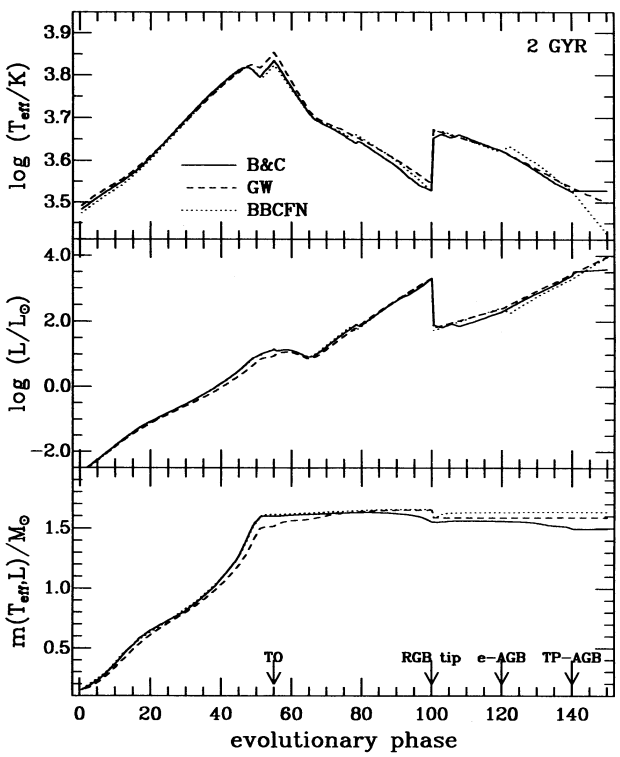

FIG. 5.—Stellar temperature, luminosity, and mass as a function of evolutionary phase along the isochrone of a 2 Gyr old, instantaneous-burst stellar population with solar metallicity in the B&C, BBCFN, and GW models. Phase 55 corresponds to the main-sequence turnoff, phase 100 to the RGB tip, phase 120 to the base of the early-AGB, phase 140 to the base of the TP-AGB, and phase 150 to the end of the TP-AGB.

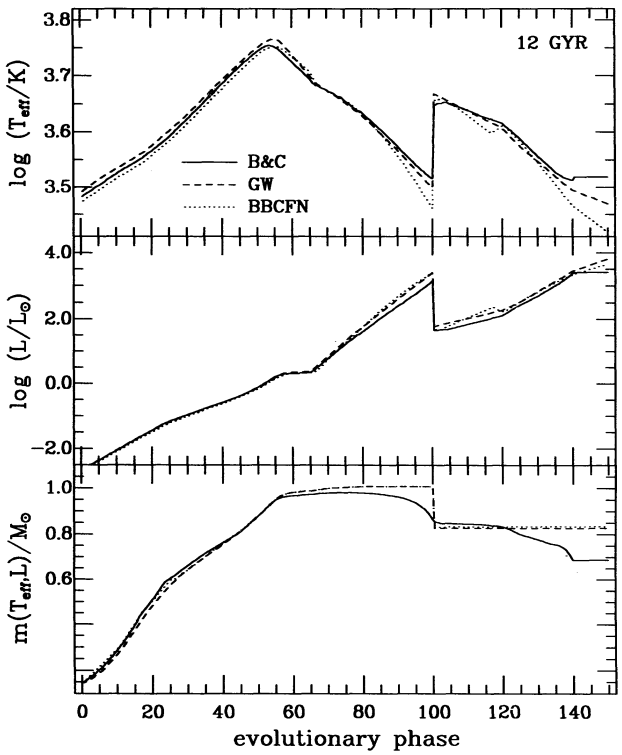

FIG. 6.—Same as Fig. 5, but for an age of 12 Gyr

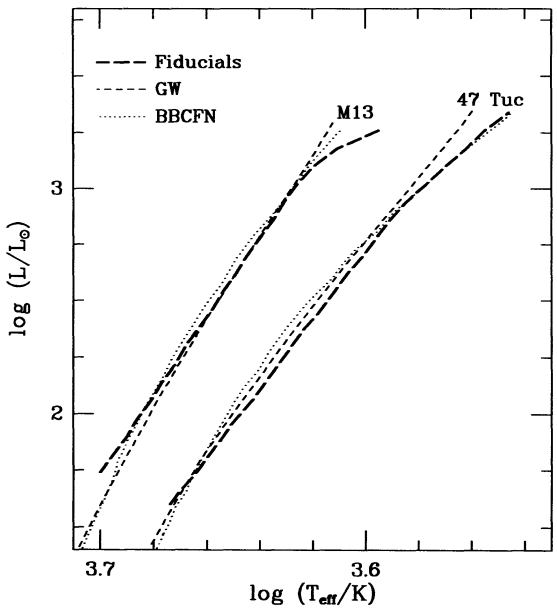

FIG. 7.—Comparison of the BBCFN and GW theoretical isochrones with RGB fiducials for the globular clusters M13 and 47 Tuc from Frogel, Persson, & Cohen (1981). The model isochrones are computed at an age of 15 Gyr. Those compared to the M13 fiducial have the metallicity [Fe/H] = −1.5, and compared to the 47 Tuc fiducial the metallicity [Fe/H] = −0.7. Except for the 0.02 dex difference on the upper RGB, the largest model-fiducial temperature mismatch is 65 K.

in the GW models. This effect persists at 12 Gyr, when the turnoff mass is about 0.9 $M_\odot$ and overshooting is not included in any model. The main reason for this difference in temperature appears to be the older radiative opacities used by GW, and hence the different calibration of the mixing length parameter (see the discussion by Bressan et al. 1993). Differences in the opacities used by B&C and BBCFN are also likely to be part of the reason for the different temperatures of upper-RGB and early-AGB stars in these models. However, we cannot decouple here this effect from the influence of other differences between the models: BBCFN include overshooting in convective envelopes; B&C include the effect of mass loss on stellar evolution, as is revealed by the masses of post–main-sequence stars in Figures 5 and 6; the two models use different values of Y; and they rely on different treatments of convection beyond the helium flash (see below). The various isochrones also differ in the properties of TP-AGB stars. The tip of the AGB is nearly twice as bright in the theoretical prescriptions of GW and BBCFN than in the empirical determination of B&C and is 15% cooler in the BBCFN model than in the GW model.

Such modest differences in the predicted isochrones explain why all models could be tested successfully against color-magnitude diagrams of observed star clusters. Figure 7 shows an example of comparison in the theoretical H-R diagram of model isochrones versus giant branch fiducials for two well-studied globular clusters, M13 and 47 Tuc (from Frogel, Persson, & Cohen 1981). The 15 Gyr isochrones of the BBCFN and GW models with [Fe/H] = −1.5 and −0.7 match the overall temperature and slope of the observed RGBs qualitatively well. Since the difference in temperature between the giant branches of the two clusters corresponds to a difference of 0.8 dex in [Fe/H], the 65 K difference in model isochrone temperature at mid-RGB for 47 Tuc translates into a 0.1 dex change in inferred metallicity. By GW's 3/2 rule for integrated light (see § 1 above), this implies a change of up to 0.15 dex in inferred age. Fortunately, this is likely to be an overestimate of the true errors because, for instance, the BBCFN isochrone for 47 Tuc is hottest at midbranch but coolest at the tip. Such differences will tend to compensate. We note that a 65 K difference in RGB star temperature can have measurable effects on the integrated light, since it corresponds to a change in $V-K$ color of 0.15 mag at 4000 K, 0.23 mag at 3800 K, and 0.40 mag at 3500 K (see § 4 below).

The photometric predictions of the models depend critically on the number of stars in each evolutionary phase along the isochrones. Figures 8*a* and 9*a* show the number distribution of stars δN as a function of evolutionary phase for the 2 Gyr and 12 Gyr isochrones, respectively, normalized to a total of 10^6 $M_\odot$ of stars produced during the burst. Differences in the rate at which stars leave the main-sequence turnoff, dN_{TO}/dt, lead to constant offsets in $\log \delta N$ at phases larger than 55 between the models. At 2 Gyr, we find that dN_{TO}/dt is the same to within 15% for all models, while at 12 Gyr, it is about 60% smaller in the BBCFN model than in the B&C and GW models. These mild differences do not explain the large discrepancies in $\log \delta N$ beyond the main sequence between the models in Figures 8*a* and 9*a*. At 2 Gyr, the GW isochrone contains an order of magnitude more subgiant stars than the B&C and BBCFN isochrones. These stars live longer in the GW model because their main-sequence progenitors, which do not experience overshooting, consume less hydrogen. Moreover, at both 2 and 12 Gyr, the GW isochrones contain a factor of about 2 more stars on the upper RGB than the BBCFN and B&C isochrones. We suspect that this mainly results from the older radiative opacities used by GW (see, for example, Table 6 of Bressan et al. 1993). However, other effects could be involved which we cannot trace back (e.g., a different helium content of

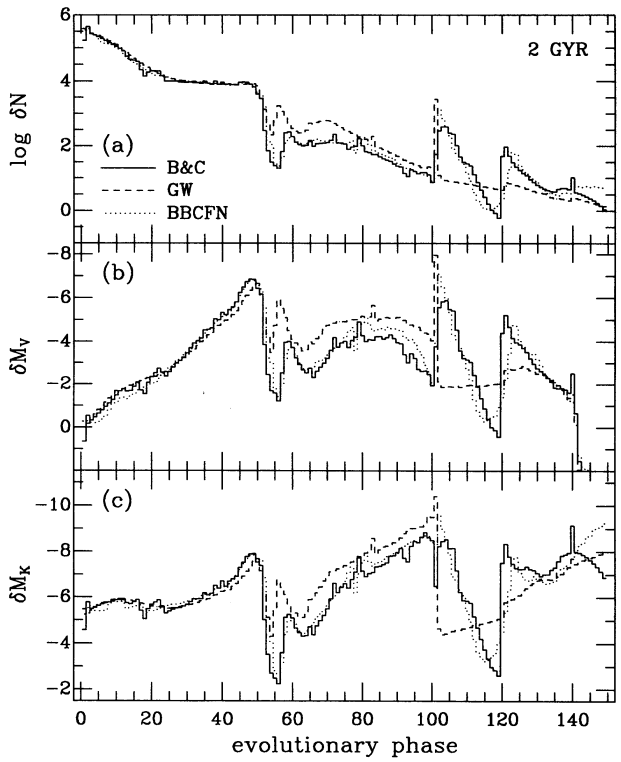

FIG. 8.—(*a*) Number distribution of stars as a function of evolutionary phase along the isochrone of a 2 Gyr old, instantaneous-burst stellar population with solar metallicity in the B&C, BBCFN, and GW models. The distributions correspond to a Salpeter IMF with lower an upper cutoffs $m_L = 0.15\ M_\odot$ and $m_U = 2\ M_\odot$, respectively, normalized to a total of $10^6\ M_\odot$ of stars produced during the burst. (*b*) and (*c*) Contributions to the absolute V and K magnitudes by stars in various evolutionary phases, as inferred from the number distributions in (*a*) and the stellar temperatures and luminosities in Fig. 5 using for all models the spectral calibrations of B&C.

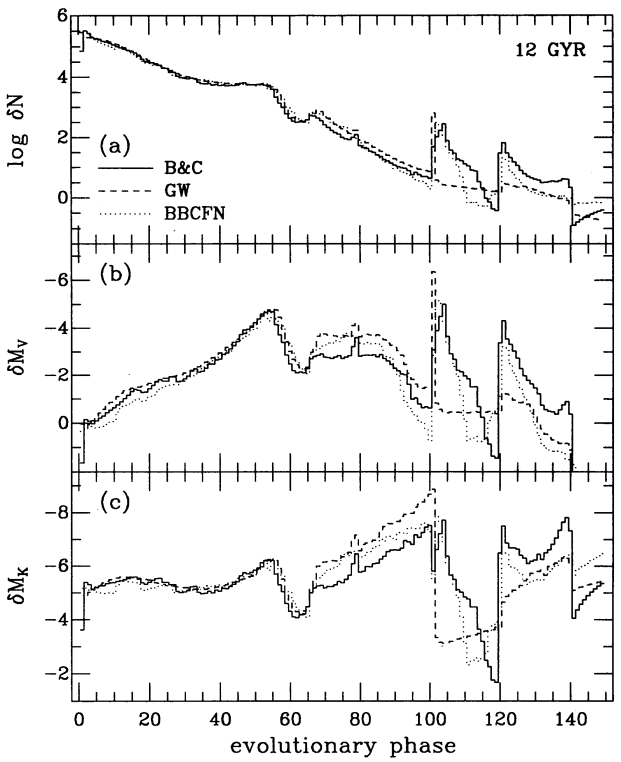

FIG. 9.—Same as Fig. 8, but for an age of 12 Gyr

the stellar envelopes). Similarly, the differences in δN between the B&C and BBCFN models must result from the differences outlined above in the input physics, although the separate influence of each parameter at play cannot be isolated here. The larger number of core-helium burning and early-AGB stars in the B&C model with respect to the BBCFN model probably results from a combination of the different Y values, different treatments of convection, and different approaches to a problematic instability near core-helium exhaustion (see also § 5.4 below). Since GW reduced the entire core-helium burning phase to a pointlike clump, the corresponding δN distribution shows a sharp peak in both Figures 8*a* and 9*a*. The B&C and GW isochrones contain similar numbers of TP-AGB stars, although with slightly different distributions, because the total lifetimes of these stars are the same in both models (Bedijn 1988). In contrast, TP-AGB stars are a factor of 2–5 more numerous in the BBCFN model.

We can now estimate the implications of these differences in stellar evolution prescription for the photometric predictions of the models by using a common spectral library to calibrate all theoretical isochrones. The stellar contributions δM_V and δM_K to the integrated V and K absolute magnitudes obtained using common spectral calibrations by B&C (see § 2.1) are shown as a function of evolutionary phase in Figures 8*b*, 8*c*, 9*b*, and 9*c*. As expected, hot stars tend to produce most of the V light and cool stars most of the K light, but important differences exist among the models. These differences can be illustrated more clearly by plotting cumulative distributions of flux as a function of evolutionary phase, i.e., $C(F, p) = \int_0^p F(p)dp$, where p is the evolutionary phase and $F(p) \propto 10^{-0.4M(p)}$. In Figures 10 and 11 we show $C(F_{\rm bol})$, $C(F_V)$, and $C(F_K)$ as a function of evolutionary phase for the 2 Gyr and 12 Gyr isochrones, respectively. The distributions are normalized in such a way that for the B&C isochrones C is unity at $p = 150$. In view of the arguments presented above, the differences illustrated by Figure 8–11 can be summarized as follows. First, the inclusion by B&C and BBCFN of convective overshooting implies a difference of about 15% at 2 Gyr in the distribution of the V light on the upper main sequence with respect to the GW models. Second, the various differences in opacities, mass loss, helium abundance, and the treatment of convection among the models imply large differences in the light contributed by post–main-sequence stars. In the GW model, RGB and core-helium burning stars produce about 20% more V light and about 30% more K light than in the BBCFN model. The difference with respect to the B&C model is about 10% greater. The compensating excesses of RGB and helium-burning stars in the B&C and BBCFN models conspire to producing roughly similar amounts of integrated V and K light prior to the TP-AGB phase. However, the long lifetimes of TP-AGB stars in the prescription adopted by BBCFN implies that 20% more of the integrated K light is produced by these cool, luminous stars at 2 Gyr.

Summing the contributions to the light by stars along the isochrones yields the integrated photometric properties of the model stellar populations. In Figure 12 we show the integrated $B-V$ and $V-K$ colors and the mass-to-visual light ratio, M/L_V, at ages between 1 and 18 Gyr. This figure is similar to Figure 1, except that a common spectral library has now been used to compute the integrated colors from the B&C, BBCFN, and GW theoretical isochrones. The differences between the

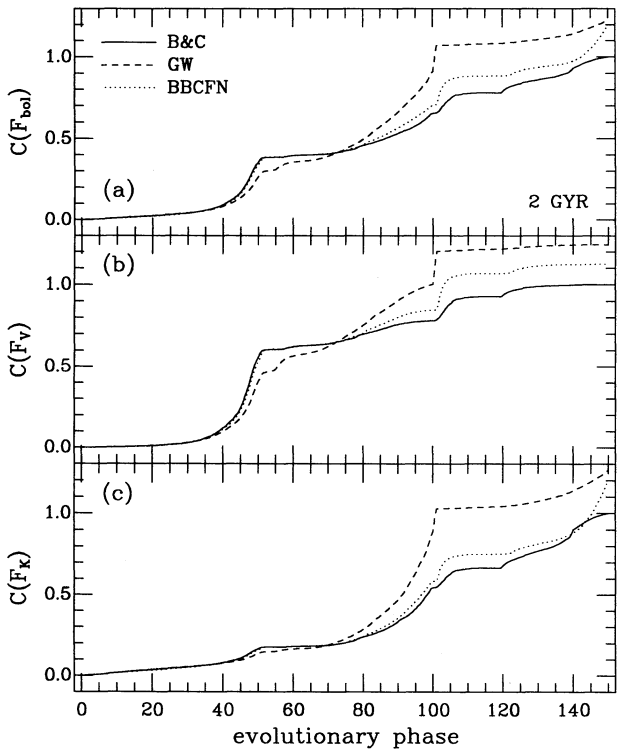

FIG. 10.—Cumulative integrals of the (*a*) bolometric flux, (*b*) *V* flux, and (*c*) *K* flux for a 2 Gyr old, instantaneous burst stellar population as a function of evolutionary phase along the isochrone. This is the cumulative version of Fig. 8. The integrals are normalized in such a way that for the B&C isochrone *C* is unity at phase number 150.

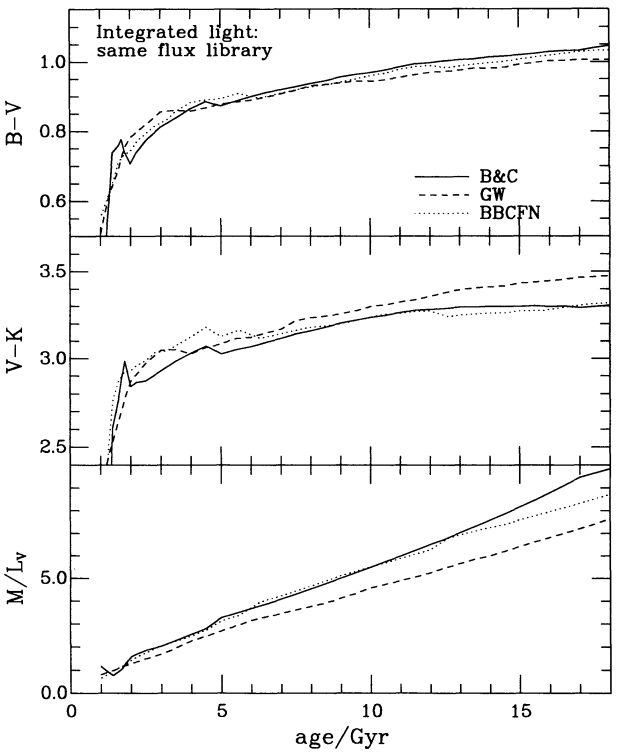

FIG. 12.—Evolution of the $B-V$ and $V-K$ colors and mass-to-V-band light ratio M/L_V of an instantaneous-burst stellar population with solar metallicity computed using the theoretical isochrones of the B&C, BBCFN, and GW models and the spectral calibrations of the B&C model. All models have the Salpeter IMF with lower and upper cutoffs $m_L = 0.15\ M_\odot$ and $m_U = 2\ M_\odot$, respectively.

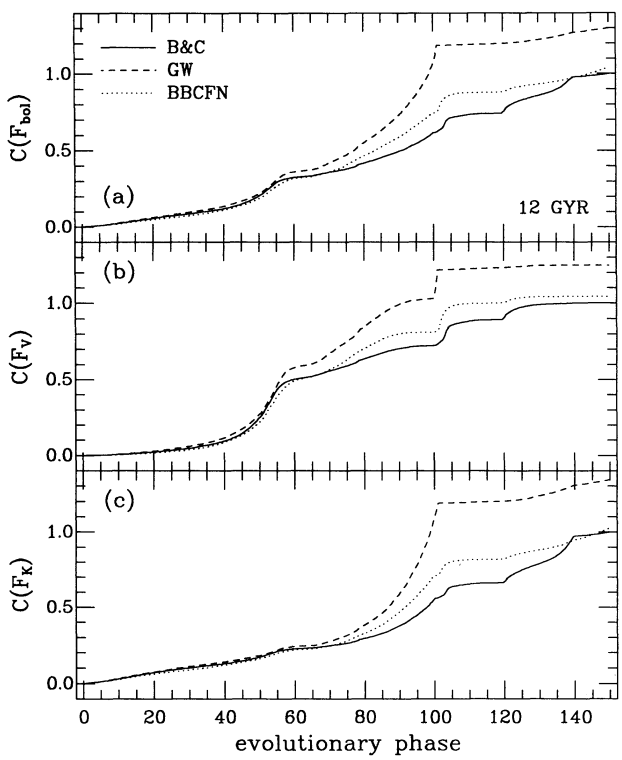

FIG. 11.—Same as Fig. 10, but for an age of 12 Gyr

predictions of the various models in Figure 12 can be interpreted in terms of the differences identified above in stellar evolution prescriptions. In particular, the evolution of the $B-V$ color agrees within 0.04 mag in the three models. The GW model is slightly bluer at ages greater than about 8 Gyr because the core-helium burning phase, which in this model is reduced to a single clump, occurs at slightly higher temperature than in the B&C and BBCFN models (Fig. 6). Discrepancies between the models are much larger in the evolution of the $V-K$ color. At ages greater than 8 Gyr, the $V-K$ color is redder by up to 0.2 mag in the GW model than in the B&C and BBCFN models because cool stars on the upper RGB produce a larger fraction of the integrated *K* light. This also causes the mass-to-light ratio to be roughly 20% smaller in the GW model. The reason why M/L_V becomes larger in the B&C model than in the BBCFN model at ages over 13 Gyr is that the difference in δN between these models remains the same on the RGB but decreases significantly in the core-helium burning and early-AGB phases, implying a reduction of the integrated light in the B&C model. The significantly redder evolution of the $V-K$ color at ages less than about 7 Gyr in the BBCFN model with respect to the B&C model results primarily from the different treatment of TP-AGB stars. To illustrate this, we show in Figure 13 the analog of Figure 12 when ignoring TP-AGB stars in all models. A comparison of Figures 12 and 13 reveals that TP-AGB stars redden the $V-K$ color of the BBCFN model by an amount that decreases from about 0.2 mag at an age of 2 Gyr to less than 0.1 mag at an age of 18 Gyr. In contrast,

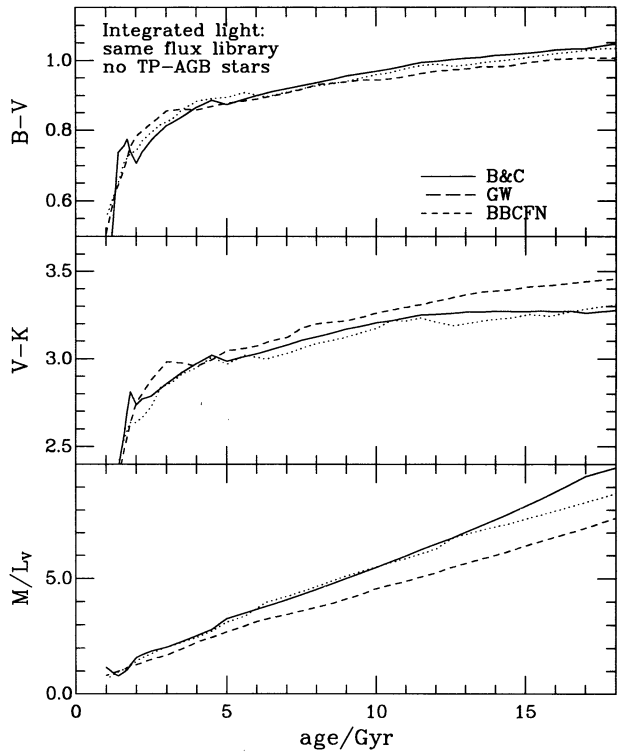

FIG. 13.—Same as Fig. 12, but after removing TP-AGB stars in all the isochrones.

TP-AGB stars do not affect significantly the integrated photometric properties of the B&C and GW models at ages greater than 2 Gyr.[4] In fact, for this reason, the photometric predictions of the BBCFN model without TP-AGB stars in Figure 13 nearly agree with those of the B&C model computed using the Padua tracks and including TP-AGB stars in Figure 1.

By comparing Figure 12 with Figure 1, we can now estimate the amount of the discrepancies in the photometric predictions of the models caused solely by differences in stellar evolution prescriptions. This comparison reveals that the bluer evolution of the $B-V$ color in the B&C model in Figure 1 with respect to the GW and BBCFN models cannot be attributed to differences in stellar evolution, and hence, it should result from differences in spectral calibrations (see § 4). On the other hand, much of the discrepancy in the evolution of the $V-K$ color between the three models appears to result from the different prescriptions for stellar evolution. Figure 12 shows that more than two-thirds of the difference in $V-K$ color between the B&C and GW models in Figure 1 results from the large number of upper RGB stars in the GW isochrones. Furthermore, the different prescriptions for TP-AGB stars account for nearly half the difference in $V-K$ color between the B&C and BBCFN models at ages around 5 Gyr in Figure 1, the magnitude of this effect then diminishing at greater ages. Figure 12 also shows that the different stellar evolution prescriptions account for nearly all of the offset in the predicted M/L_V ratio between the GW model and the B&C and BBCFN models in Figure 1. Hence, many, but not all, of the discrepancies in the photometric predictions of the three models appear to result from differences in stellar evolution prescriptions alone.

[4] The contribution by TP-AGB stars is expected to be larger at ages around 1 Gyr. See, for example, B&C.

4. INFLUENCE OF THE SPECTRAL CALIBRATIONS

We estimate here the effect of changes in spectral calibrations on the photometric predictions of population synthesis models. By analogy with our approach in the previous section, we now fix the stellar evolution prescription (theoretical isochrones) and compute the colors obtained by using alternatively the B&C, BBCFN, and GW spectral calibrations. As outlined in § 2, all authors first compile stellar spectra from which colors are calculated using selected filter passbands. B&C use a library constructed mostly from observational spectra, calibrated to agree in color and bolometric correction with the Johnson (1966) color-color tables. GW and BBCFN use Kurucz (1992) model atmospheres for stars warmer than 4000 K. The Kurucz models were included without further empirical calibration. For cooler stars, GW adopted alternative theoretical spectra for M giants in the infrared, on which he pasted observational spectra at optical wavelengths. The cool dwarf sequence in his model is an extrapolation from giants. No empirical corrections were applied by GW in this procedure. BBCFN, on the other hand, assembled for cool stars a library of observational spectra. In what follows, we first examine the resulting differences in color-temperature scale, color-color calibrations, and bolometric corrections between the models and then estimate the effect of these differences on the photometric predictions. As before, the reader interested only in the main conclusions of our analysis is referred to the last paragraph of the section.

Figure 14 shows the $B-V$ and $V-K$ colors assigned to dwarf and giant stars as a function of effective temperature in the B&C, BBCFN, and GW models. Also shown are the

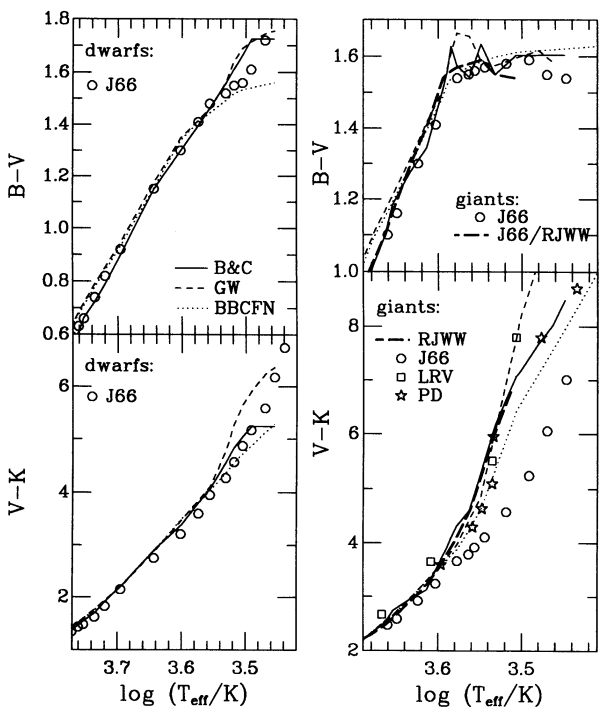

FIG. 14.—$B-V$ and $V-K$ colors adopted as a function of effective temperature for dwarf and giant stars in the B&C, BBCFN, and GW models. Also shown are the Johnson (1966) calibrations (J66), the $V-K$ color-temperature scales of Ridgway et al. (1980, RJWW), Lançon & Rocca-Volmerange (1992; LRV; see text for detail), and BBCFN (PD), and the $B-V$ color-temperature scale inferred from the Ridgway et al. $V-K$ color-temperature scale and the Johnson $B-V$ color-$V-K$ color calibration (J66/RJWW).

average colors of stars in the solar neighborhood tabulated by Johnson (1966). Dwarfs with temperatures $T_{\rm eff} \gtrsim 4000$ K ($\log T_{\rm eff} \gtrsim 3.60$) are assigned $V-K$ colors that are similar in all models and in agreement with the Johnson calibration, but the assigned $B-V$ colors are about 0.06 mag redder in the GW and BBCFN models than in the Johnson calibration and the B&C models. This offset is caused by a known limitation of the Kurucz (1992) model atmospheres for stars in this temperature and gravity regime (GW; Gratton & Carretta 1995). The colors of dwarfs cooler than 3500 K ($\log T_{\rm eff} \lesssim 3.54$) show much stronger discrepancies from a model to another and with respect to the empirical relations. However, this is not critical for photometric predictions because such cool dwarfs contribute only little to the integrated light (see, e.g., Figs. 6 and 11).

The colors assigned to giants are more crucial because these stars can dominate the blue-to-visual light of old stellar populations. In the B&C model, colors for giants were calibrated using the empirical $V-K$ color-temperature scale of Ridgway et al. (1980) that extends down to $\log T_{\rm eff} = 3.51$ (type M6 III). The scale is shown in Figure 14, together with the original $V-K$ color-temperature scale of Johnson (1966) and the $V-K$ color-temperature scale inferred from the $H-K$ color-temperature scale of Lançon & Rocca-Volmerange (1992). This scale was estimated for stellar types earlier than M7 by converting the $H-K$ colors in Table 1 of Lançon & Rocca-Volmerange (1992) into $V-K$ colors using the color-color table of Bessell & Brett (1988) and then drawing a by-eye fit through the results (the coolest star in the Lançon & Rocca-Volmerange sample, a Mira variable of type M8.5 and amplitude ΔV of more than 4 mag, was ignored because of its uncertain $V-K$ color). For giants hotter than 4500 K ($\log T_{\rm eff} \gtrsim 3.65$), the $B-V$ offset of about 0.06 mag in the BBCFN and GW models with respect to the empirical relations and the B&C model is caused again by a known limitation of the Kurucz (1992) model atmospheres (GW; Gratton & Carretta 1995). For giants cooler than $\log T_{\rm eff} = 3.51$, the $V-K$ colors can differ by more than 1 mag between the GW and B&C models as it is not constrained by observations.[5] BBCFN relied on a different $V-K$ color-temperature scale for giants, also shown in Figure 14, which they determined by means of comparisons with observed color-magnitude diagrams. The corresponding $V-K$ colors are almost 1 mag bluer than the Ridgway et al. scale for stars with temperatures around 3300 K ($\log T_{\rm eff} = 3.52$) and 1 mag bluer than the $V-K$ colors adopted by B&C for cooler stars.

We can compare more extensively model colors versus empirical colors by using as observational reference the Johnson (1966) color-color calibrations for dwarfs and giants. We relate colors to effective temperature by adopting the Johnson (1966) scale for dwarfs and the Ridgway et al. (1980) scale for giants. The line labeled J66/RJWW in Figure 14 illustrates the empirical $B-V$ color-temperature scale then obtained for giants. In Figure 15 we show differences of several other model colors *minus* the Johnson colors computed in this way as a function of $V-K$ color for dwarfs and giants. The model colors were computed at the tabulated Johnson (or Ridgway et al.) temperatures using suitable surface gravities (see Table 2 of GW). The dwarfs contributing most significantly to the integrated light are those with colors in the range $1 \lesssim V-K \lesssim 2$. The giants contributing most significantly to the integrated blue-to-visual light are those bluer than $V-K \approx 3$. Figure 15 shows several interesting features. First, as expected by construction, the B&C colors follow the Johnson colors reasonably well, with modest excursions which are caused by the discrete nature of the B&C flux library. Second, the BBCFN and GW colors are very similar, which is also expected since the underlying Kurucz flux library is the same. In particular, the deviation of about 0.06 in $B-V$ color for giants bluer than $V-K = 3$ and for warm dwarfs is virtually identical in both the BBCFN and GW models. This deviation is important because it propagates to integrated colors nearly unattenuated, for example when warm giants dominate the integrated blue-to-visual light. Third, BBCFN and GW do not agree well in $U-V$ color. The main reason for this is the adoption of different U filter passbands. Fourth, very cool stars (i.e., with $V-K \gtrsim 4$) show wide dispersions in most colors between authors and with respect to the Johnson (1966) calibrations. This effect is magnified by the fact that the colors of these cool stars are extremely sensitive to temperature, thus small errors in temperature scale lead to large errors in color. The cool dwarfs contribute very little to integrated light, but the cool giants contribute significantly at wavelengths longer than 1 μm.

The absolute magnitude scale of the models and the relative weights of stars in the integrated light rely on the adopted bolometric corrections. Figure 16 shows BC_V, the stellar bolometric correction in the V band, as a function of effective temperature in the B&C, BBCFN, and GW models for dwarf and giant stars. These relations were calibrated using absolute bo-

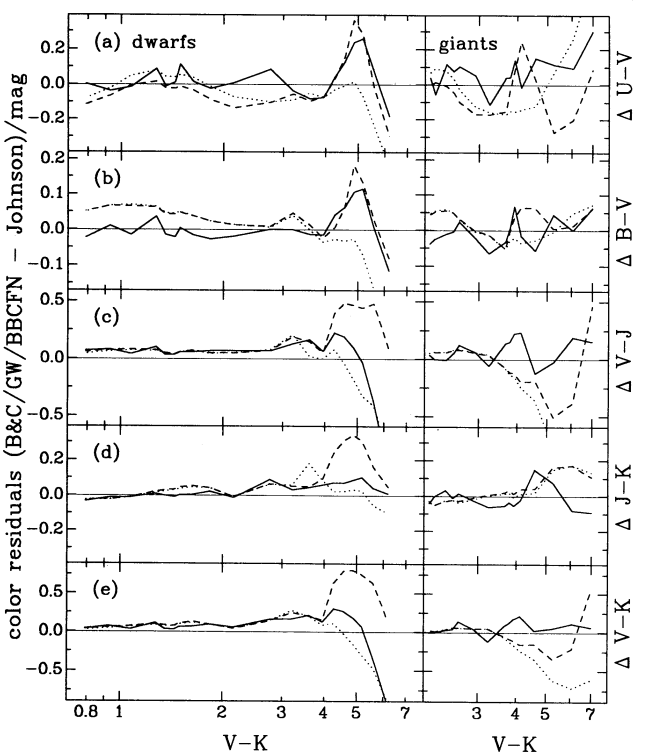

FIG. 15.—Model minus empirical $UBVJK$ color residuals for solar neighborhood dwarf and giant stars. As in previous figures, the solid line is B&C, the dashed line GW, and the dotted line BBCFN. See discussion in the text.

[5] TP-AGB stars in the B&C model were treated separately. Stars on the lower TP-AGB were assigned the colors of Mira Ceti, $B-V = 1.56$ and $V-K = 5.88$, and stars on the upper TP-AGB the colors of IK Tau, $B-V = 1.93$ and $V-K = 14.13$, regardless of temperature. The adopted V bolometric corrections are $BC_V = -3.27$ for lower TP-AGB stars and $BC_V = -10.94$ for upper TP-AGB stars (see Appendix of Charlot & Bruzual 1991).

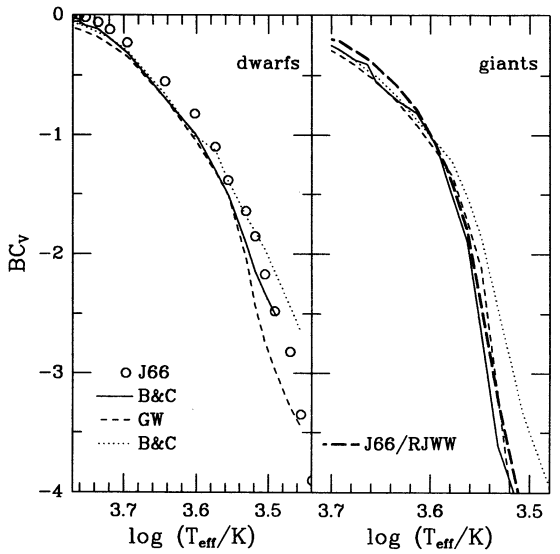

FIG. 16.—V-band bolometric correction, $BC_V = M_{bol} - M_V$, adopted as a function of effective temperature in the B&C, BBCFN, and GW models. Also shown are the Johnson (1966) calibrations for dwarfs and giants, using for giants the Ridgway et al. (1980) $V-K$ color-temperature scale.

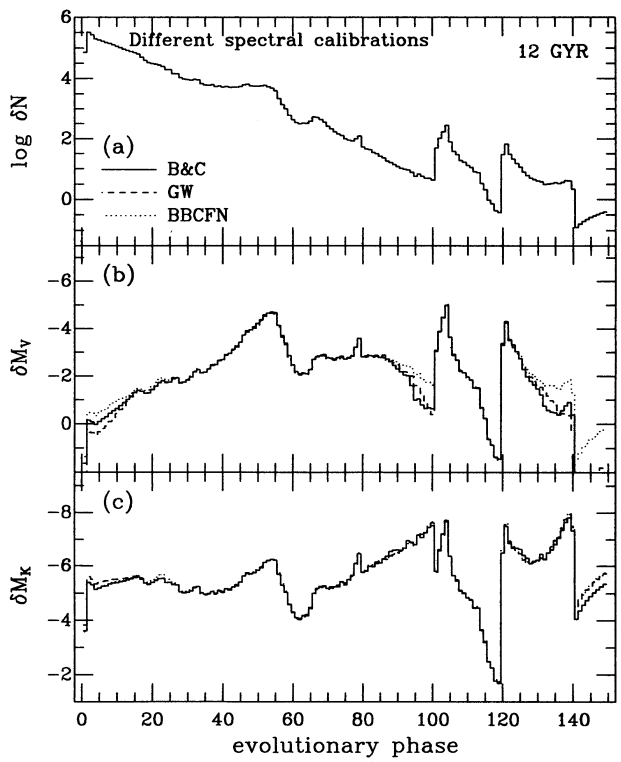

FIG. 17.—(*a*) Number distribution of stars as a function of evolutionary phase along the isochrone of a 12 Gyr old, instantaneous-burst stellar population with solar metallicity in the B&C model. The distribution corresponds to a Salpeter IMF with lower and upper cutoffs $m_L = 0.15\ M_\odot$ and $m_U = 2\ M_\odot$, respectively, normalized to a total of $10^6\ M_\odot$ of stars produced during the burst. (*b*) and (*c*) Contributions to the absolute V and K magnitudes by stars in various evolutionary phases, as inferred from the number distribution in (*a*) and the stellar temperatures and luminosities along the B&C isochrone in Fig. 6 using the spectral calibrations of the B&C, BBCFN, & GW models.

lometric magnitudes and V-band bolometric corrections for the Sun listed in Table 1 (i.e., at $\log T_{eff\odot} \approx 3.76$). We also indicate in Figure 16 the empirical bolometric corrections tabulated by Johnson (1966) using his color-temperature scale for dwarfs and that of Ridgway et al. (1980) for giants. For stars hotter than about 4000 K ($\log T_{eff} \gtrsim 3.60$), the color-temperature scales are well defined, and the bolometric corrections from the various models in Figure 16 are similar and lie within 0.1 mag of the empirical expectations. For cooler stars, however, the deviations are larger. The BBCFN model appears to predict systematically larger bolometric corrections for dwarfs and giants, indicating V magnitudes systematically brighter than in the B&C and GW models at fixed bolometric luminosity. For giants, the offset with respect to the B&C and GW models, which better follow the empirical relation, increases from about 0.1 mag at 3800 K ($\log T_{eff} \approx 3.58$) to more than 1 mag at 3300 K ($\log T_{eff} \approx 3.52$). For cool dwarfs the difference in BC_V between the BBCFN and GW models is similar to that for cool giants, while the B&C model, with intermediate values, is closer to the Johnson calibration. Regardless of the small offset in normalization at the Sun temperature, these significant and large differences in BC_V are again caused by discrepancies in both $V-K$ color-temperature scale and stellar spectra among the models.

The above differences in spectral calibrations have implications for the predicted photometric properties of the models. We first evaluate the changes imparted to the distribution of stellar fluxes inferred from a fixed theoretical isochrone. Figure 17 shows the contributions δM_V and δM_K of stars in various evolutionary phases to the integrated V and K absolute magnitudes of a 12 Gyr old stellar population, as obtained by applying alternatively the spectral calibrations of the B&C, BBCFN, and GW models to the B&C theoretical isochrone. The variations in δM_V and δM_K from a model to another can be readily interpreted in terms of the differences in spectral calibrations identified previously after consulting the distribution of stellar effective temperatures along the isochrone (Fig. 6). Since main-sequence and core-helium burning stars are warm, their predicted contribution to the V and K light are similar in all models. The differences in the contribution by cool stars on the upper RGB and AGB are more significant. As expected, the stars are brighter in the V band in the BBCFN model than in the B&C and GW model. The predicted K magnitudes are comparable in all models because at fixed temperature, the $V-K$ color is bluer in the BBCFN model. Figure 17 also shows that a crossing of the color-temperature scales for giant stars around $\log T_{eff} \approx 3.52$ in the B&C and GW models (Fig. 14) causes the V magnitude computed using the GW calibrations to transit on the upper RGB and early AGB from brighter than the one computed using the B&C calibrations into fainter. On the TP-AGB, stars have the brighest V magnitude in the BBCFN model because the V bolometric correction is the smallest. Cool stars on the lower main sequence also present significant deviations in V magnitude among the models. Again, these stars contribute negligibly to the integrated light.

By analogy with our approach in § 3, we now sum the contributions to the light by stars along the isochrone and compute the integrated photometric properties of the model stellar population. Figure 18 shows the integrated $B-V$ and $V-K$ colors and the mass-to-visual light ratio, M/L_V at ages between 1 and 18 Gyr. At each age, the theoretical isochrone of the B&C model was combined with the spectral libraries of the B&C, BBCFN, and GW models to compute the integrated

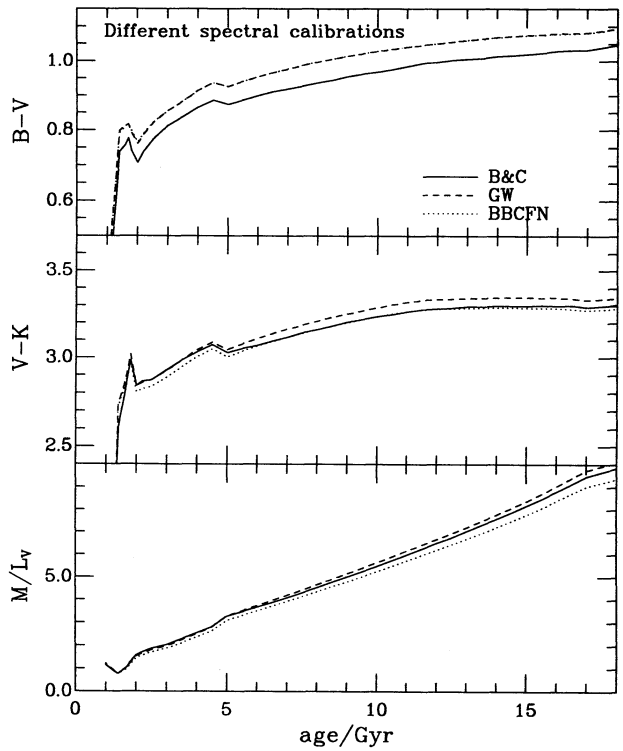

FIG. 18.—Evolution of the $B-V$ and $V-K$ colors and mass-to-visual light ratio M/L_V of an instantaneous-burst stellar population with solar metallicity computed using the theoretical isochrones of the B&C model and the spectral calibrations of the B&C, BBCFN, and GW models. The B&C model has the Salpeter IMF with lower and upper cutoffs $m_L = 0.15\ M_\odot$ and $m_U = 2\ M_\odot$, respectively.

photometric properties. Figure 18 reveals that the differences in the photometric calibrations of the various models have only a small effect on the integrated colors. However, this similarity results in part from the conspiracy of more substantial discrepancies compensating each other. Most remarkably, the large differences in the adopted bolometric corrections and color-temperature scale for giants in the B&C and BBCFN models conspire into producing a nearly identical evolution of the $V-K$ color. As a result, the only apparent differences between the three models in Figure 18 are a less than 10% spread in M/L_V and 0.05 mag offsets in colors: the BBCFN and GW models that rely on the Kurucz (1992) model atmospheres predict $B-V$ colors systematically redder than the B&C model; and the GW model, in which the redder $V-K$ colors of cool stars are not counterbalanced by larger bolometric corrections, predicts $V-K$ colors systematically redder than the B&C and BBCFN models.

5. SUMMARY AND DISCUSSION

5.1. *Summary*

A comparison of Figure 1 with Figures 12 and 18 summarizes the separate effects of stellar evolution and spectral calibrations on the photometric predictions of the models. This confirms that the 0.05 mag discrepancy in predictions of the $B-V$ color can be entirely attributed to a known limitation of model atmospheres. Furthermore, differences in spectral calibrations introduce relatively small discrepancies in the predicted $V-K$ color (about 0.05 mag) and mass-to-visual light ratio (about 5%–10%). In contrast, differences in stellar evolution prescriptions can produce deviations of up to 0.2 mag in the predicted $V-K$ color and of 15%–20% in the predicted mass-to-visual light ratio. We point out that these estimates are indicative only of the uncertainties inherent in the three models considered here. As we have shown, larger discrepancies were found to sometimes counteract each other in these models, conspiring into a misleading agreement.

Hence, the main uncertainties in modern population synthesis models appear to originate from the underlying stellar evolution theory, the color-temperature scale of giant stars, and, for nonsolar abundances in particular, the flux libraries. These conclusions also apply to population synthesis models other than those considered here because the limitations are intrinsic to the fundamental assumptions underlying the models (e.g., Arimoto & Yoshii 1987; Guiderdoni & Rocca-Volmerange 1987; Buzzoni 1989; Fritze von Alvensleben & Gerhard 1994). In the following we briefly investigate the reasons for these persistent weaknesses, reviewing current problems in spectral calibrations and in the theories of stellar structure and evolution, as well as other limitations of populations synthesis models. Finally, in § 5.8 we use our results to estimate indicative uncertainties on determinations of the age, metallicity, and mass of observed galaxies based on current population synthesis models.

5.2. *Uncertainties Linked to Spectral Calibrations*

As described in § 4, the spectral calibration of population synthesis models can be schematically divided into a color-temperature calibration and color-color, or spectral energy distribution, calibration. The most commonly used color-temperature scale for solar-metallicity G8 to M6 giants is that derived by Ridgway et al. (1980), which relates the $V-K$ color with the effective temperature derived from measurements of angular diameters by lunar occultations. Other modern temperature scales based on model atmosphere analysis or the method of total-to-infrared flux ratio agree with the Ridgway et al. scale, usually to within 50 K (Tsuji 1978; 1981; Blackwell, Lynas-Gray, & Petford 1991; Bell & Gustafsson 1989). The $V-K$ color presents itself as a nearly optimum color for temperature estimates in cool stars for two main reasons. First, the range of $V-K$ colors is large over the range of cool star temperatures, which minimizes the uncertainty caused by observational errors. Second, no study based on model atmospheres has so far indicated any significant dependence of the $V-K$ color on metallicity for temperatures in the range $4000 \lesssim T_{\rm eff} \lesssim 5000$ K, hence making the $V-K$ color useful to calibrate nonsolar metallicity stars as well. This insensitivity probably breaks down for cooler stars (Bessell et al. 1989) and for very metal poor stars (Bell & Gustafsson 1989).

Assuming that the $V-K$ color is a reliable temperature indicator for even the coolest giants (as should be the case for giants of a single metallicity and mass), the limitation of the Ridgway et al. (1980) color-temperature scale to spectral types earlier than M6 ($T_{\rm eff} \gtrsim 3300$ K) still allows unwanted uncertainties in model predictions. This can be evaluated, for instance, by consulting Figures 6 and 11 above. Stars of type M7 and M8, i.e., with $\log T_{\rm eff} \lesssim 3.50$, appear at phases 96–100 on the upper RGB and 136–140 on the upper AGB in the BBCFN isochrone at an age of 12 Gyr. Figure 11 indicates that these stars account for about 10% of the integrated K light and 0% of the integrated V light, hence contributing roughly 0.1 mag of the integrated $V-K$ colors. Since very late type stars, even if they are rare, can therefore contribute significantly to

the integrated light of old stellar populations, the nearly 2 mag uncertainty in their assigned $V-K$ color and 1 mag uncertainty in their assigned bolometric correction in the models are not negligible. The main reason for the absence of a reliable color-temperature scale at such cool temperatures is the scarcity of normal (non-Mira) giant stars of spectral types M7 and M8 in the solar neighborhood, which renders the empirical determination of their temperatures difficult, at least by means of lunar occultation.

The spectra of M giants (i.e., with $T_{\rm eff} < 3900$ K) are also difficult to model theoretically because they are blanketed mostly by molecular opacity and because their atmospheres tend to be extremely extended. This is unfortunate for the purpose of population synthesis modeling because M giants dominate the light at wavelengths redward of about 1 μm for metal-rich populations of most ages. Our understanding in this area can progress by studies of Galactic, Magellanic, and bulge M giants; the inclusion of always more realistic opacities due to water and other important molecules; a more complete determination of the color-temperature scale; and models of atmospheric structure in M giants to get reliable pressure boundary conditions for evolutionary calculations. Stellar populations of different metallicities, and even different elemental mixes, may then be eventually modeled with confidence, but this seems a long way ahead.

Several projects are underway that should help overcome at least some of the present uncertainties in the area of spectral libraries in general, and for M giants in particular. Le Borgne et al. (1995) are building an observational library encompassing a few hundred optical/infrared spectra of stars with metallicities in the range $-2.0 \lesssim [{\rm Fe/H}] \lesssim +0.5$. This project has been designed specifically to provide a full and efficient coverage of the H-R diagram for the purpose of stellar population synthesis models. Furthermore, Cuisinier et al. (1994) and Lejeune (1995) have undertaken a thorough calibration of the optical/infrared colors and temperature and metallicity scales of model atmosphere (Bessell et al. 1989; Kurucz 1992) using optical/infrared photometry and low-resolution optical spectroscopy of various samples of Galactic cluster and field stars. The sample stars so far mainly cover the metallicity range $-2.5 \lesssim [{\rm M/H}] \lesssim 0.0$, and their photometric properties show systematic deviations with respect to the predictions of model atmospheres. The goal of these studies is to determine corrections to apply to libraries of synthetic stellar spectra, especially in the range corresponding to M giants, for the specific purpose of cluster H-R diagram analyses and stellar population synthesis modeling. In addition to these comprehensive studies, Meyer et al. (1995) have recently obtained a medium-resolution spectral library covering the J and H bands for 88 solar-metallicity stars of types in the range O5–M5 and luminosity classes I–II, III, and IV–V.

These new spectral libraries will be valuable to reduce uncertainties originating from spectral calibrations in population synthesis models. It should be emphasized that accurate spectrophotometry, although challenging from beneath the Earth's atmosphere, is crucially needed for progress in this area. In addition, the solar neighborhood is missing types of stars that are expected to be common in other environments such as young but metal-poor stars, very metal rich stars of any age, and stars of solar or greater metallicity but with enhanced abundances of light elements similar to those found in the Galactic bulge and external galaxies (McWilliam & Rich 1994; Worthey, Faber, & González 1992). This lack of local calibrators increases the dependence of population synthesis modeling on theoretical model atmospheres.

5.3. *Uncertainties Linked to the Stellar Structure*

The theory of stellar evolution emerges as one of the major causes of uncertainties in populations synthesis models. There are several fundamental sources of limitation in current stellar models: atomic data (i.e., radiative opacities, heavy-element mixture, helium content, reaction rates), convection theory (i.e., mixing length, overshoot, semiconvection), mixing in radiative regions (i.e., rotational mixing, thermal diffusion, gravitational settling), and mass loss. The uncertainties associated with these different phenomena are all related together in complicated ways. As a result, the tuning of a specific parameter by fits of observed stars depends on the values adopted for all the other parameters. A complete discussion of stellar models is beyond the scope of the present paper (see, e.g., Chiosi, Bertelli, & Bressan 1992 for a more complete review). We point out here only a few general weaknesses of present models, indicating references to more detailed discussions and ongoing progress.

Stellar models are sensitive to changes in radiative opacities (e.g., Schaller et al. 1992; Bressan et al. 1993; Charbonnel & Lebreton 1993; Charbonnel et al. 1995). Several opacity tables have been published over the last few years by Rogers & Iglesias (1992), Iglesias et al. (1992), Iglesias & Rogers (1993), and Seaton et al. (1994), which aside from significant updates include different choices for the mixture of heavy elements. Alexander & Ferguson (1994) have also recently computed low-temperature radiative opacities for different chemical compositions. The inclusion of these various new calculations in stellar models have shown not only that the tuning of convection parameters depends on the adopted opacities, but also that changes in the relative fractions of heavy elements (e.g., from scaled-solar to CO-rich mixtures) can affect the lifetime, temperature, or luminosity of some model stars by (at least) 5%–10% (Schaller et al. 1992; Bressan et al. 1993; Charbonnel et al. 1995). In fact, the morphology of the turnoff and of the red giant branch in the H-R diagram are known to depend sensitively on the relative abundances of heavy elements (e.g., Renzini & Fusi Pecci 1988, and references therein). These conclusions are disturbing because grids of stellar models are generally computed assuming that the mixture of heavy elements is fixed and scales linearly with metallicity, while in reality the relative abundances of heavy elements are expected to vary even within a single star (for instance, when some elements are dredged up to the surface; see also below). In addition, as mentioned in § 5.2, the relative ratios of heavy elements, and in particular the ratio of α-elements to iron, can on average differ from the solar values in old Galactic stars and in some external galaxies (e.g., McWilliam & Rich 1994; Worthey et al. 1992).

Another complicating process has recently become the subject of a vivid debate around stellar models: the diffusion of elements inside radiative regions. This process, which has long been invoked to explain surface abundances in stars and the constraints from helioseismology, could also lead to substantial revisions of the temperatures, luminosities, and lifetimes predicted by standard models (e.g., Demarque, Deliyannis, & Sarajedini 1992; Richer, Michaud, & Proffitt 1992; Chaboyer, Demarque, & Pinsonneault 1995). For example, Stringfellow et al. (1983) find that including helium diffusion in the radiative cores of low-mass, Population II stars could reduce by 15%–25% the ages derived by isochrone fitting for old star clusters. More recent constraints from observations of lithium

abundances in halo stars suggest that the efficiency of helium diffusion is probably less than originally thought, although models including the combined effects of diffusion and rotational mixing are only starting to develop (Chaboyer, Sarajedini, & Demarque 1992; Chaboyer et al. 1995; see also Vauclair & Charbonnel 1995). It is worth mentioning here that, as pointed out by Charbonnel & Lebreton (1993), all models for the evolution of low-mass stars still suffer from the lack of a reliable equation of state (except for the solar model).

Unfortunately, comparisons with observed star clusters cannot always be used to adjust the parameters of stellar models because the solutions present some degeneracies. For example, changes in radiative opacities affect the predicted "width" of the main sequence, and in turn the favored efficiency of convective overshooting (Bressan et al. 1993, and references therein). The most recent comparisons with observations appear to favor mild overshooting in the cores of stars with masses between about 1.5 and 5 $M_{\odot}$, and little or no overshooting in lower mass stars (Bressan et al. 1993; Meynet, Mermilliod, & Maeder 1993; Demarque, Sarajedini, & Guo 1994). Another degenerate observational constraint is the ratio of enrichment in helium over that in metals, $\Delta Y/\Delta Z$. This ratio is important because it controls the initial helium abundance at fixed metallicity and the molecular weight, and hence the mass-luminosity relation and lifetimes of metal-rich stars. To illustrate this dependence, we compare in Table 2 the lifetimes from zero-age main sequence to RGB tip for low-mass stars with two different compositions (Fagotto 1994; Fagotto et al. 1994b): $Z = 0.05$, $Y = 0.352$ ($\Delta Y/\Delta Z \approx 2.5$) and $Z = 0.05$, $Y = 0.4$ ($\Delta Y/\Delta Z \approx 3.5$). This variation in $\Delta Y/\Delta Z$ is small compared to the range allowed by the observations, $2 \lesssim \Delta Y/\Delta Z \lesssim 7$ (Lequeux et al. 1979; Pagel et al. 1992; Renzini 1994). Table 2 indicates that at fixed mass, the stellar lifetimes increase by up to 40% when Y is changed from 0.4 to 0.352, or that, equivalently, at fixed age the turnoff mass increases by roughly 0.1 $M_{\odot}$. Remarkably, these large variations do not impact dramatically on the age derived by isochrone fitting because the increase in turnoff mass when Y decreases is also balanced by a drop in luminosity and temperature. In fact, the GW model predicts a modulation of only 15% in the inferred age at [Fe/H] = +0.5 if $\Delta Y/\Delta Z$ is set to 0.0 instead of 2.7. This relative insensitivity is comforting, but one must be aware of the implications of the adopted rate of helium to metals enrichment on other properties of stellar populations which depend on actual mass (e.g., mass-to-light ratio).

5.4. *Advanced Stages of the Stellar Evolution*

The advanced stages of evolution, which are crucial to the predictions of population synthesis models because of the high corresponding stellar luminosities, suffer from other profound uncertainties. In § 3 we have exemplified the role of three uncertain phenomena in the evolution of stars beyond the main sequence: mass loss on the red giant branch, the treatment of convection during core-helium burning, and thermal pulses of AGB stars. We defer the discussion of mass loss along the RGB to the next subsection, since the main effect of this uncertain phenomenon appears to be the nonstandard evolution of core-helium burning stars.

TABLE 2

DEPENDENCE OF HYDROGEN-BURNING AND RGB LIFETIME ON HELIUM CONTENT FOR $Z = 0.05$

Initial Mass/$M_{\odot}$	$t(Y = 0.352)$/Gyr	$t(Y = 0.400)$/Gyr
0.8	27.04	18.34
0.9	17.24	11.57
1.0	11.00	7.81
1.1	7.59	5.37

The treatment of convection during core-helium burning has traditionally been a subject of great attention because it strongly affects the relative numbers of RGB, core-helium burning, and AGB stars that can be observationally measured. As summarized by Renzini & Fusi Pecci (1988), accurate observations of 15 metal-poor globular clusters in the Milky Way halo require that the amount of helium burnt in the cores of stars on the horizontal branch be larger than the amount available at the RGB tip, the most natural candidates for helium refuel at the core boundary being semiconvection (an actual theoretical prediction) and overshooting. A characteristic instability near core-helium exhaustion, referred to as "breathing convection," can also lengthen the core-helium burning lifetime (Castellani et al. 1985). The models of Castellani et al. (1985), however, which include semiconvection in addition to the breathing convection instability, predict core-helium burning lifetimes longer than observed (Renzini & Fusi Pecci 1988). This result has generally been interpreted as an indication that breathing convection may be an artifact of the idealized algorithm used to handle core mixing (e.g., Bressan, Bertelli, & Chiosi 1986; Bressan et al. 1993). The recent calculations by Charbonnel et al. (1995) used in the Geneva tracks option of the B&C model include breathing convection but no semiconvection nor overshooting. These new tracks, which also differ from previous calculations in the prescriptions for opacities, heavy-element mixture, and mass loss, are being tested against observations (Charbonnel 1995; see also Charbonnel et al. 1995 for more detail).

One of the least understood phases of stellar evolution is the luminous, double-shell–burning regime that low- and intermediate-mass stars undergo on the upper AGB. The phase is characterized by periodic thermal pulses of the He shell and by heavy, but probably episodic mass loss (Zijlstra et al. 1992, and reference therein). Stars then build up a circumstellar shell that reradiates a fraction of their light in the infrared. From the perspective of population synthesis models, TP-AGB stars are important not only because they have very high infrared luminosities, but also because the final core mass at envelope ejection has direct implications for the integrated ultraviolet light of old stellar populations (see § 5.5). The details of the evolution, however, are very uncertain, and an empirical determination of the lifetime and luminosities of TP-AGB stars still seems preferable over simplified theoretical prescriptions (e.g., Vassiliadis & Wood 1993; see the recent reviews by Habing 1995a, b).

Observations by the *Infrared Astronomical Satellite* have led to the schematic view that TP-AGB stars probably evolve from a Mira phase, in which the star has a thin envelope and a pulsation period of a few hundred days, into a strong OH-maser emission phase, in which the envelope has become thicker and the pulsation period can exceed a thousand days (e.g., Bedijn 1988). Since the luminosity correlates well with the hydrogen-exhausted core mass (Paczyński 1970), and in turn with main-sequence progenitor mass, more massive stars in this interpretation evolve naturally toward more luminous OH/IR stars with longer pulsation periods. In the least massive stars, on the other hand, the Mira and OH/IR phases would

occur at similar luminosities (e.g., Fig. A1 of B&C; see also the classification of TP-AGB stars in terms of main-sequence progenitor mass by Habing 1995a, b). We note that the maximum luminosity of TP-AGB stars is difficult to determine observationally because of the small number statistics and of the contamination of observational samples by red supergiants.

Theoretical models of TP-AGB stars are slowly developing, but they still suffer from serious uncertainties. Among the most critical processes involved are the efficiency of carbon dredge-up that influences the core growth and the abundance of the envelope, the driving mechanism and efficiency of mass loss that influences the final core mass and maximum luminosity, the effect of metallicity, and the parameters of convection (Renzini & Voli 1981; Bowen & Willson 1991; Blöcker & Schönberner 1991; Vassiliadis & Wood 1993; Groenewegen & de Jong 1994). Several observational constraints can be used to calibrate the models, but most are difficult to measure and suffer from large uncertainties as well. These include the core-mass luminosity relation (Paczyński 1970), the period-luminosity relation (Hughes & Wood 1990), the observed ratio of carbon-rich to oxygen-rich stars, observational estimates of the mass-loss rate, and the possible relation between period and mass loss rate (Epchtein, Le Berte, & Lépine 1990; Vassiliadis & Wood 1993; but see Habing 1995b).

Both observational and theoretical approaches have been adopted to include TP-AGB stars in population synthesis models. In the B&C model, these stars were implemented semi-empirically using samples of Galactic stars analyzed by Herman & Habing (1985) and Herman, Burger, & Phoenix (1986), but the evolutionary timescales, taken from Bedijn (1988), are uncertain. BBCFN adopted a simple theoretical prescription for the evolution of TP-AGB stars with an empirically motivated law of mass loss (Reimers 1975). The uncertainties introduced by the treatment of TP-AGB stars alone on the predictions of population synthesis models have been illustrated in § 3 (see Figs. 12 and 13).

Future infrared sky surveys are expected to clarify some aspects of the evolution of TP-AGB stars, including the AGB maximum luminosity and number ratios of stars of different compositions and with different mass-loss rates (see Le Berte et al. 1994; Wood 1994). It is worth recalling that some properties of TP-AGB stars appears to depend sensitively on metallicity. The influence of metallicity on the appearance of TP-AGB stars appear to depend sensitively on metallicity. The influence of metallicity on the appearance of TP-AGB stars can be illustrated by comparing available samples of stars in the Galaxy and in the Large and Small Magellanic Clouds, although age differences also exist among these samples. The ratio of carbon-rich (C-type) to oxygen-rich (bluer, M-type) stars is found to increase significantly from about 0.01 in Baade's window, to about 2 in the LMC and nearly 50 in the SMC. (Blanco, Blanco, & McCarthy 1978). Furthermore, as expected if the dust-to-gas ratio in the envelopes correlates with metallicity, stars with high mass-loss rates appear to be more obscured in the Galactic bulge than in the LMC (Habing 1995b). These important variations let us envision persistent uncertainties in the inclusion of TP-AGB stars in population synthesis models even after larger samples of Galactic and Magellanic Clouds stars become available. As a slightly more positive prospect, Lançon & Wood (1995) are obtaining low-resolution, optical/infrared spectra of a sample of TP-AGB stars in the Galaxy and LMC that should be valuable to better represent these stars in population synthesis models.

5.5. *The Hot Star Problem*

Space observations in the ultraviolet have revealed a high-temperature stellar component in elliptical galaxies and spiral bulges which has generated much interest in recent years (e.g., Burstein et al. 1988; Ferguson & Davidsen 1993; see also Greggio & Renzini 1990; Magris & Bruzual 1993; Bressan et al. 1994; Dorman, Rood, & O'Connell 1993; Bertola et al. 1995; Dorman, O'Connell, & Rood 1995). In summary, the observed spectral shape of the "excess" ultraviolet flux in elliptical galaxies and spiral bulges suggests that it is most likely produced by a combination of very hot post-AGB stars on their way to becoming white dwarfs, and a category of old, slightly warmer stars whose nature is still very uncertan, commonly called "extreme blue horizontal branch" (EHB) stars. Bertola et al. (1995) estimate by directly counting resolved post-AGB stars in the bulge of M31 that these could account for about 20%–50% of the total ultraviolet flux. Despite rapid progress on the observational front, the ultraviolet emission from old stellar populations remains a challenge for current population synthesis models. We now briefly mention some of the reasons for this weakness.

The first difficulty affecting the modeling of the ultraviolet emission from old stellar populations is that the emission from post-AGB stars cannot be evaluated with confidence as it strongly depends on the highly uncertain mass of the stars leaving the AGB (§ 5.4). The dependence of the ultraviolet flux on the relation between main-sequence and post-AGB mass (the "initial-final mass" relation) can be estimated, for example, by comparing the models of Bruzual & Charlot (1993) to those of Magris & Bruzual (1993), or by inspecting integrated spectra computed for different mass-loss rates by Bressan et al. (1994). This dependence is also illustrated in Table 3, where we list the integrated $1550-V$ color of an instantaneous burst stellar population computed at various ages with the Bressan et al. (1994) code for two initial-final mass relations: that of Weidemann (1987) and that obtained by using the Reimers (1975) formula with $\eta = 0.45$ to describe mass loss on the RGB and AGB. At fixed initial mass, the first relation predicts a smaller final mass than the second one. Table 3 shows that both relations give the same $1550-V$ color at an age of 16 Gyr. However, at younger ages the color predicted by the Weidemann relation can be more than a magnitude bluer than that obtained with the Reimers parameterization. The reason for this is that lower mass post-AGB stars are slightly less luminous but live much longer than their counterparts of higher mass (e.g., Schönberner 1983). This high uncertainty on the ultraviolet emission from post-AGB

TABLE 3

DEPENDENCE OF THE INTEGRATED ULTRAVIOLET EMISSION ON THE PRESCRIPTION FOR MASS LOSS FOR $Z = 0.02$

Age/Gyr	$(1550-V)^a$	$(1550-V)^b$
3.....	6.1	6.8
5.....	5.6	6.7
7.....	5.0	6.5
10.....	4.4	6.1
16.....	3.7	3.7

[a] Adopting the initial-final mass relation of Weidemann 1987.

[b] Adopting the Reimers 1975 formula for mass loss on the RGB and AGB ($\eta = 0.45$).

stars dramatically affects the interpretation of the ultraviolet excess from old stellar populations.

The other source of ultraviolet emission in elliptical galaxies and spiral bulges, the EHB component, is even less understood. These stars could be normal, old horizontal branch stars of very low metallicity (e.g., Lee 1994), old horizontal branch stars of metallicity slightly larger than solar which have lost much of their envelope during the previous RGB phase because of enhanced mass loss (e.g., Dorman et al. 1995; see also Greggio & Renzini 1990), or old horizontal branch stars of very high metallicity ($Z \lesssim 0.1$ for $\Delta Y/\Delta Z \gtrsim 2.5$) which suffered normal mass loss on the RGB (e.g., Bressan et al. 1994). The first alternative has not been thoroughly investigated, but preliminary analysis indicates that the strength of the excess ultraviolet light would require giant elliptical galaxies in dense environments to be nearly 20 Gyr old, in conflict with current opinion on the age of the universe (Park & Lee 1995; see also Dorman et al. 1995). This hypothesis may also not match quantitatively an observed trend of increasing ultraviolet flux with stronger Mg absorption (Burstein et al. 1988). The suggestion by Dorman et al. (1995; see also Greggio & Renzini 1990) follows from indirect measurements of mass loss on the RGB by comparing the masses of turnoff and clump stars in two old, open clusters of solar metallicity, M67 and NGC 6791 (Tripicco, Dorman, & Bell 1993; Liebert, Saffer, & Green 1994). Carraro et al. (1995), however, show that mass determination of clump stars by isochrone fitting is highly uncertain and requires extremely high precision of the distance modulus (0.025 mag to achieve a 5% uncertainty in the mass). In fact, an equally good fit to the turnoff and clump stars of M67 can be obtained with negligible mass loss on the RGB. Alternatively, the ultraviolet emission of even the most powerful elliptical galaxies could be produced by a very small fraction ($\lesssim 2\%$ in mass) of very high metallicity ($Z \approx 0.1$ for $\Delta Y/\Delta Z \approx 2.5$) stars (Bressan et al. 1994). Such stars, however, have never been observed, although the above conditions can be met, for instance in the Galactic bulge (McWilliam & Rich 1994). These large uncertainties in the origin of the EHB component imply that studies of the hot star population in elliptical galaxies and spiral bulges remain a mostly empirical problem in which stellar evolution calculations provide essential guidance, rather than a predictable phenomenon suitable for precise evolutionary synthesis.

5.6. *Binarism*

The analysis of a sample of solar neighborhood stars in the Yale Bright Star Catalog is compatible with a binary frequency of over 50% (Eggleton, Fitchett, & Tout 1989). Binary stars should therefore ideally be included in population synthesis models. An expected consequence of binaries is to give rise (by coalescence) to "blue stragglers," i.e., stars appearing brighter than the turnoff on an extension of the main sequence, although blue stragglers are also expected to result from other phenomena (Stryker 1993). The progeny of binary stars is not expected to affect significantly the luminosity function of bright stars in old stellar populations (Rich, Mould, & Graham 1993). Binaries also produce Type Ia supernovae, and hence they are an important factor in the chemical enrichment of galaxies. In addition, mass transfer from close companions can lead to chemically peculiar stars (i.e., Ba II stars and Tc-deficient S and MS stars; Johnson, Ake, & Ameen 1993). In view of the uncertainties already outlined in the previous paragraphs and of the many additional assumptions required to include the effects of binary stars, the neglect of these stars in most current population synthesis models has so far been a known but tolerated deficiency.

5.7. *Synthesis of Young Stellar Populations*

We have deliberately avoided in the present paper to discuss the synthesis of young ($\lesssim 1$ Gyr old) stellar populations to remain in the overlapping regime of the different stellar evolution calculations most widely used in population synthesis models (the VandenBerg, Yale, Geneva, and Padova libraries). The presence of stars more massive than $2\,M_\odot$ in stellar populations younger than 1 Gyr introduces other types of uncertainties, which include the photoionizing radiation and energy output from massive stars, the relative numbers of red and blue supergiants, the evolution of Wolf-Rayet (W-R) stars, and the rate of Type II supernovae. We mention here only some of the main characteristics and uncertainties of models of young stellar populations and refer the reader to the recent comparative studies by García-Vargas, Bressan, & Leitherer (1995c) and Charlot (1996) for more detail.

The evolution of a massive star is not well understood because current models do not include the coupling of the interior physics with that of the outer atmosphere, whose expansion though a wind is known to greatly affect the subsequent evolution of the star and its surrounding medium. Instead, the strength of the stellar wind is usually parameterized in a simple way and roughly calibrated against available observations (see the recent reviews by Chiosi et al. 1992 and Maeder & Conti 1994). The most extensive calculations of evolutionary tracks for massive stars suitable to population synthesis modeling are those of the Geneva and Padova groups. Both cover a wide range of masses (up to $120\,M_\odot$) and metallicities (see references in § 2). The global properties of the two calculations appear to be almost the same: the evolution of stars with masses between $10\,M_\odot$ and $30\,M_\odot$ is extremely sensitive to the details of internal mixing (convective or diffusive) and affects the relative ratio of red to blue supergiants; and the evolution of more massive stars is controlled essentially by mass loss that causes their progeny (the so-called hypergiants) to lose part or all of their hydrogen-rich envelope and to appear as bare He nuclei commonly identified with W-R stars. The internal structure and mass-loss rate of massive stars also depend sensitively on the abundances of heavy elements (e.g., Maeder & Conti 1994).

The spectrophotometric properties of young stellar populations have been investigated traditionally by including tracks and spectra for massive stars in the models in a similar way as for low- and intermediate-mass stars (e.g., BBCFN, B&C, and references therein). A few recent models for young stellar populations also include the influence of massive stars on their environment, which allows more detailed comparisons with observations of star-forming galaxies (e.g., Cerviño & Mas-Hesse 1994; Vacca 1994; Leitherer & Heckman 1995; García-Vargas, Bressan, & Díaz 1995a, b). These models predict not only integrated colors and continuum spectra, but also optical/infrared emission-line spectra and the radiative and kinetic energy output from young stellar populations. However, such predictions suffer from the large uncertainties in the underlying stellar evolution prescription (i.e., the Geneva or Padova tracks for various opacities and mass-loss prescriptions) and in the model atmospheres for massive stars (i.e., LTE or non-LTE, static or expanding envelopes, etc., Kurucz 1979, 1992; Clegg & Middlemass 1987; Schmutz, Leitherer, & Gruenwald

1992). The recent studies by García-Vargas et al. (1995c) and Charlot (1996) indicates that the main source of uncertainties in the models is the underlying stellar evolution prescription.

5.8. *Applications of Current Population Synthesis Models*

The above discussion motivates a reevaluation of the predictions of current population synthesis models. Ideally, one would like to estimate the uncertainties on derivations of the properties of observed galaxies using such models by varying only one free parameter at a time. The limited number of available models does not allow us to do so. Therefore, we evaluate here some indicative uncertainties that should be attached to the predictions of modern population synthesis models based on the dispersion in the properties of the models considered in the previous sections. The main interest in population synthesis models is generally the determination of the age, metallicity, and mass of galaxies from their observed spectral energy distributions. For simplicity, we consider here idealized galaxies containing a single generation of stars with unique metallicity and no dust. We first fix the metallicity to solar and estimate the uncertainties on determinations of absolute ages, age differences, and absolute masses from observed colors and luminosities. The GW 3/2 rule, d log age/d log $Z \approx 3/2$ at fixed observed colors and optical spectral indices, can then be used to estimate the dispersion in metallicity determinations at fixed age from that in age determinations at fixed metallicity. Even for idealized galaxies defined as above, the uncertainties in age and metallicity determinations will increase, as indicated by the GW 3/2 rule, if both quantities are allowed to vary. For real galaxies containing several generations of stars with different metallicities, determinations of age, metallicity, and mass of the various components will be far more uncertain. In addition, the presence of dust in real galaxies can complicate these determinations because the effects of dust on broad-band colors are almost undistinguishable from those of age and metallicity (e.g., Fig. 2 above).

To evaluate the uncertainties in the determination of absolute ages and masses for solar-metallicity stellar populations older than about 1 Gyr (the limit imposed by the 2 $M_\odot$ upper cutoff of the IMF used by GW), we list in Table 4 the mean and standard deviation as a function of age of the $B-V$ and $V-K$ colors and mass-to-visual light ratio computed using four different models: the B&C model with either the Geneva or Padua tracks, the BBCFN model, and the GW model. Indicative uncertainties on galaxy ages derived from observed $B-V$ and $V-K$ colors can be inferred directly from this table. For example, an idealized galaxy with solar metallicity and $B-V = 0.89 \pm 0.01$ (to allow for minimal observational errors) would be assigned an age of about 5 ± 2 Gyr (40% accuracy), and a galaxy with $B-V = 1.00 \pm 0.01$ an age of about 12 ± 3 Gyr (25% accuracy). These accuracies in the derived ages could be further reduced by correcting the BBCFN and GW predictions for a known offset in $B-V$ color (see § 4). Age estimates based on the $V-K$ color are more uncertain, as expected from the larger dispersion of the models predictions in this color. For example, the age assigned to a galaxy with $V-K = 3.25 \pm 0.01$ would range from 7 to over 17 Gyr ($\gtrsim$40% accuracy). Table 4 can also be used to estimate the uncertainties in the mass derived for an idealized galaxy with solar metallicity from its luminosity, although this requires some information about the age and an additional assumption about the IMF. Since M/L_V is roughly proportional to age, the minimum uncertainty on the absolute mass is therefore similar to the uncertainty on the absolute age, i.e., about 25%–40%, to which must be added the uncertainty on the assumed IMF.

The determination of relative ages between two galaxies for which a difference in color or luminosity has been measured suffers from similar uncertainties. To quantify this, we compute the derivatives with respect to age of the $B-V$ and $V-K$ colors and mass-to-visual light ratio for the four models considered above using the time evolution of these properties shown in Figure 1. The results are presented in Figure 19, and the mean and dispersion of the derivatives over all four models are listed as a function of age in Table 4. The usefulness of these quantities for determining are relative ages between two different stellar populations can be illustrated as follows. For an observed color difference $\delta(B-V)$, the implied difference in age is $\delta t \approx \delta(B-V)\ [\partial(B-V)/\partial t]^{-1}$. The relative dispersion in $\partial(B-V)/\partial t$, which ranges between 10% and 70% depending on

TABLE 4

INDICATIVE UNCERTAINTIES IN THE PREDICTIONS OF THREE STELLAR POPULATION SYNTHESIS MODELS[a,b]

Age	$B-V$	$V-K$	M/L_V	$\partial(B-V)/\partial t$	$\partial(V-K)/\partial t$	$\partial(M/L_V)/\partial t$
2.....	0.74 ± 0.07	2.87 ± 0.14	1.47 ± 0.17	0.090 ± 0.023	0.054 ± 0.082	0.597 ± 0.154
3.....	0.84 ± 0.03	2.99 ± 0.11	1.99 ± 0.19	0.068 ± 0.032	0.106 ± 0.063	0.480 ± 0.083
4.....	0.88 ± 0.03	3.06 ± 0.14	2.50 ± 0.20	0.035 ± 0.024	0.060 ± 0.060	0.546 ± 0.087
5.....	0.89 ± 0.03	3.07 ± 0.13	3.16 ± 0.30	0.012 ± 0.012	0.008 ± 0.037	0.584 ± 0.126
6.....	0.91 ± 0.03	3.10 ± 0.12	3.63 ± 0.28	0.015 ± 0.012	0.026 ± 0.040	0.493 ± 0.145
7.....	0.93 ± 0.03	3.14 ± 0.10	4.08 ± 0.35	0.018 ± 0.002	0.045 ± 0.014	0.426 ± 0.057
8.....	0.95 ± 0.03	3.18 ± 0.11	4.52 ± 0.39	0.016 ± 0.004	0.037 ± 0.015	0.448 ± 0.048
9.....	0.96 ± 0.03	3.22 ± 0.10	4.98 ± 0.44	0.016 ± 0.005	0.034 ± 0.008	0.449 ± 0.043
10.....	0.98 ± 0.02	3.25 ± 0.10	5.42 ± 0.44	0.014 ± 0.003	0.027 ± 0.008	0.449 ± 0.068
11.....	0.99 ± 0.02	3.27 ± 0.10	5.87 ± 0.50	0.015 ± 0.002	0.024 ± 0.014	0.469 ± 0.086
12.....	1.00 ± 0.02	3.29 ± 0.11	6.35 ± 0.58	0.007 ± 0.005	0.004 ± 0.027	0.540 ± 0.132
13.....	1.01 ± 0.02	3.30 ± 0.11	6.91 ± 0.66	0.007 ± 0.004	0.008 ± 0.016	0.493 ± 0.128
14.....	1.02 ± 0.02	3.30 ± 0.12	7.36 ± 0.73	0.009 ± 0.002	0.009 ± 0.013	0.465 ± 0.109
15.....	1.03 ± 0.02	3.31 ± 0.13	7.85 ± 0.81	0.009 ± 0.003	0.009 ± 0.011	0.498 ± 0.121
16.....	1.04 ± 0.02	3.31 ± 0.14	8.35 ± 0.92	0.008 ± 0.002	0.005 ± 0.011	0.522 ± 0.158
17.....	1.05 ± 0.02	3.32 ± 0.14	9.28 ± 1.06	0.005 ± 0.002	0.002 ± 0.012	0.529 ± 0.165

[a] For an instantaneous burst stellar population of solar metallicity and with a Salpeter IMF from 0.15 $M_\odot$ to 2 $M_\odot$.

[b] Units are age in Gyr, colors in mag, M/L_V in $M_\odot\ L_{\odot V}^{-1}$, color derivatives in mag Gyr^{-1}, and $\partial(M/L_V)/\partial t$ in $M_\odot\ L_{\odot V}^{-1}$ Gyr^{-1}.

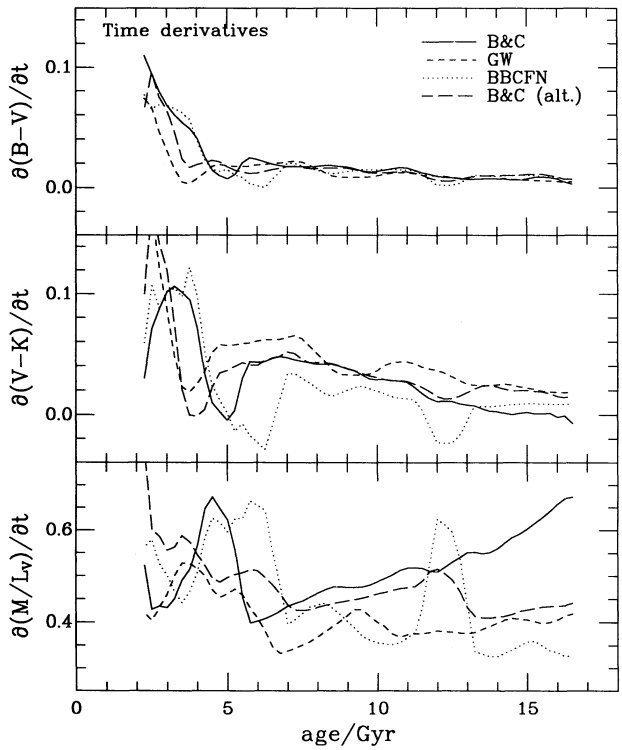

FIG. 19.—Time derivatives of the $B-V$ and $V-K$ colors (in mag Gyr^{-1}) and of the mass-to-visual light ratio M/L_V (in $M_\odot L_{\odot V}^{-1}$ Gyr^{-1}) for an instantaneous-burst stellar population of solar metallicity computed with the B&C, BBCFN, and GW models and with the Bruzual & Charlot (1995) models using the Padua tracks (B&C alt.). This is the time derivative version of Fig. 1.

the age in Table 4, is therefore also roughly the relative dispersion in δt. Hence, for example, the difference in age between two galaxies with colors $B-V \approx 0.89 \pm 0.01$ and 1.00 ± 0.01 will be, using Table 4, $\delta t \approx 0.11 \times 0.016^{-1} \times (1 \pm 0.31)^{-1} \approx 7 \pm 2$ Gyr. Using the GW 3/2 rule, the above uncertainties on age determinations at fixed solar metallicity can be reexpressed as rough uncertainties on metallicity determinations at fixed age. We infer that, for example, the metallicity of a 5 Gyr old, idealized galaxy containing a single generation of stars could be determined to within 25% using current population synthesis models.

As a final note, spectral indices which measure individual absorption features are becoming a ubiquitous prediction of population synthesis models as they seem to provide a way to partially isolate age effects from metallicity effects, almost independently of the presence of dust (GW). In particular, Balmer features in combination with metallic features have been used to derive mean ages for early-type galaxies (e.g., González 1993; Bressan et al. 1995; Worthey, Trager, & Faber 1995). To roughly estimate the sensitivity of such age determinations on the population synthesis modeling, we have computed the evolution of several optical spectral indices for an instantaneous burst stellar population using alternatively the GW and BBCFN theoretical isochrones, the single flux library of GW, and the index fitting functions of Worthey et al. (1994). The average uncertainty on the absolute ages derived from spectral indices was then found to be of approximately 25% at old ages ($\gtrsim 10$ Gyr), i.e., similar to the uncertainty obtained by using the $B-V$ color for dust-free galaxies. The results of § 4 indicate that the additional uncertainty introduced by the choice of spectral calibrations should be fairly small. However, the additional uncertainty in index fitting functions remains to be assessed (see, e.g., Chavez, Malagnini, & Morossi 1995). In any event, differences in abundance ratios in real galaxies appear to introduce substantially more uncertainty into age determinations than do models (Worthey et al. 1995). Moreover, caution must be paid in deriving galaxy ages from integrated narrow band indices because of the great sensitivity of some indices to the last episode of star formation alone. For example, even if only a few percent of the total luminous mass of a galaxy is involved in a recent episode of star formation superimposed on a much older population, the age inferred for the whole galaxy from the strengths of the Hβ or Hδ indices will be significantly younger (e.g., Charlot & Silk 1994; Bressan et al. 1995).

We thank M. Fall, A. Omont, R. Peletier, A. Sarajedini, D. Silva, and especially G. Bruzual and C. Charbonnel for helpful discussions. S. C. acknowledges the hospitality of the Institute for Theoretical Physics, UCSB, where parts of this project were completed. This research was supported in part by the NSF under grant PHY-94-07194 and in part by NASA through grant HF-1066.01-94A awarded by the Space Telescope Science Institute, which is operated by the Association of Universities for Research in Astronomy, Inc., for NASA under contract NAS5-26555.

REFERENCES

Alexander, D. R., & Ferguson, J. W. 1994, ApJ, 437, 879
Alongi, M., Bertelli, G., Bressan, A., & Chiosi, C. 1991, A&A, 244, 95
Alongi, M., Bertelli, G., Bressan, A., Chiosi, C., Fagotto, F., Greggio, L., & Nasi, E. 1993, A&AS, 97, 851
Arimoto, N., & Yoshii, Y. 1987, A&A, 173, 23
Bedijn, P. J. 1988, A&A, 205, 105
Bell, R. A., & Gustafsson, B. 1989, MNRAS, 236, 653
Bertelli, G., Bressan, A., & Chiosi, C. 1985, A&A, 150, 33
Bertelli, G., Bressan, A., Chiosi, C., Fagotto, F., & Nasi, E. 1994, A&AS, 106, 275 (BBCFN)
Bertola, F., Bressan, A., Burstein, D., Buson, L. M., Chiosi, C., & di Serego Alighieri S. 1995, ApJ, 438, 680
Bessell, M. S. 1990, PASP, 102, 1181
Bessell, M. S., & Brett, J. M. 1988, PASP, 100, 1134
Bessell, M. S., Brett, J. M., Scholz, M., & Wood, P. R. 1989, A&AS, 77, 1
———. 1991, A&AS, 89, 335
Blackwell, D. E., Lynas-Gray, A. E., & Petford, A. D. 1991, A&A, 245, 567
Blanco, B. M., Blanco, V. M., & McCarthy, M. F. 1978, Nature, 271, 638
Blöcker, T., & Schönberner, D. 1991, A&A, 244, L43
Böhm-Vitense, E. 1972, A&A, 17, 335
Bowen, H. G., & Willson, L. A. 1991, ApJ, 375, L53
Bressan, A., Bertelli, G., & Chiosi, C. 1986, Mem. Soc. Astron. Ital., 57, 411
Bressan, A., Chiosi, C., & Fagotto, F. 1994, ApJS, 94, 63
Bressan, A., Chiosi, C., & Tantalo, R. 1995, A&A, submitted
Bressan, A., Fagotto, F., Bertelli, G., & Chiosi, C. 1993, A&AS, 100, 647
Bruzual A., G. 1983, ApJ, 273, 105
Bruzual A., G., & Charlot, S. 1993, ApJ, 405, 538
———. 1995, ApJ, in preparation (B&C)
Burstein, D., Bertola, F., Buson, L. M., Faber, S. M., Lauer, T. R. 1988, ApJ, 328, 440
Burstein, D., Faber, S. M., Gaskell, C. M., & Krumm, N. 1984, ApJ, 287, 586
Buser, R., & Kurucz, R. L. 1978, A&A, 70, 555
Buzzoni, A. 1989, ApJS, 71, 817
Carraro, G., Girardi, L., Bressan, A., & Chiosi, C. 1995, A&A, in press
Castellani, V., Chieffi, A., Pulone, L., & Tornambé, A. 1985, ApJ, 296, 204
Cerviño, M., & Mas-Hesse, J. M. 1994, A&A, 284, 749
Chaboyer, B., Demarque, P., & Pinsonneault, M. H. 1995, ApJ, 441, 876
Chaboyer, B., Sarajedini, A., & Demarque, P. 1992, ApJ, 394, 515
Charbonnel, C. 1995, private communication
Charbonnel, C., & Lebreton, Y. 1993, A&A, 280, 666
Charbonnel, C., Meynet, G., Maeder, A., Schaller, G., & Schaerer, D. 1995, A&AS, submitted
Charlot, S., in From Stars to Galaxies, ed. C. Leitherer, V. Fritz-von Alvensleben, & J. Huchra (ASP Conf. Ser.), in press

Charlot, S., & Bruzual A., G. 1991, ApJ, 367, 126
Charlot, S., & Silk, J. 1994, ApJ, 432, 453
Chavez, M., Malagnini, M. L., & Morossi, C. 1995, ApJ, 440, 210
Chiosi, C., Bertelli, G., & Bressan, A. 1992, ARA&A, 30, 235
Clegg, R. E. S., & Middlemass, D. 1987, MNRAS, 228, 759
Code, A. D., Davis, J., Bless, R. C., & Hanbury Brown, R. 1976, ApJ, 203, 417
Cohen, J. G. 1982, ApJ, 258, 143
Crampin, J., & Hoyle, F. 1961, MNRAS, 122, 27
Cuisinier, F., Buser, R., Acker, A., Cayrel, R., Jasniewicz, G., & Fresneau, A. 1994, A&A, 285, 943
Davidge, T. J. 1992, ApJ, 397, 457
Demarque, P., Deliyannis, C. P., & Sarajedini, A. 1992, in Observational Tests of Cosmological Inflation, ed. T. Shanks et al. (Dordrecht: Kluwer), 111
Demarque, P., Sarajedini, A., & Guo, X.-J. 1994, ApJ, 426, 165
Dorman, B., O'Connell, R. W., & Rood, R. T. 1995, ApJ, 442, 105
Dorman, B., Rood, R. T., & O'Connell, R. W. 1993, ApJ, 419, 596
Eggleton, P. P., Fitchett, M. J., & Tout, C. A. 1989, ApJ, 347, 998
Epchtein, N., Le Berte, T., & Lépine, J. R. D. 1990, A&A, 227, 82
Fagotto, F. 1994, Ph.D. thesis, University of Padua
Fagotto, F., Bressan, A., Bertelli, G., & Chiosi, C. 1994a, A&AS, 100, 647
———. 1994b, A&AS, 104, 365
———. 1994c, A&AS, 105, 29
Ferguson, H. C., & Davidsen, A. F. 1993, ApJ, 408, 92
Flower, P. J. 1977, A&A, 54, 31
Fluks, M. A., Plez, B., Thé, P. S., de Winter, D., Westerlund, B. E., & Steenman, H. C. 1994, A&AS, 105, 311
Fritze von Alvensleben, U. A., & Gerhard, O. E. 1994, A&A, 285, 751
Frogel, J. A., Persson, S. E., Aaronson, M., & Matthews, K. 1978, ApJ, 220, 75
Frogel, J. A., Persson, S. E., & Cohen, J. G. 1981, ApJ, 246, 842
García-Vargas, M. L., Bressan, A., & Díaz, A. I. 1995a, A&A, in press
———. 1995b, A&AS, in press
García-Vargas, M. L., Bressan, A., & Leitherer, C. 1995c, in preparation
Girardi, L., Chiosi, C., Bertelli, G., Bressan, A. 1995, A&A, in press
González, J. J. 1993, Ph.D. thesis, Univ. California, Santa Cruz
Gratton, R. G., & Carretta, E. 1995, A&A, submitted
Greggio, L., & Renzini, A. 1990, ApJ, 364, 35
Green, E. M., Demarque, P., & King, C. R. 1987, The Revised Yale Isochrones and Luminosity Functions (New Haven: Yale University Observatory)
Groenewegen, M. A. T., & de Jong, T. 1994, A&A, 283, 463
Guiderdoni, B., & Rocca-Volmerange, B. 1987, A&A, 186, 1
Gunn, J. E., & Stryker, L. L. 1983, ApJS, 52, 121
Habing, H. J. 1995a, MSAI, in press
———. 1995b, ARA&A, in preparation
Herman, J., Burger, J. H., & Phennix, W. H. 1986, A&A, 167, 247
Herman, J., & Habing, H. J. 1985, Phys. Rep., 124, 255
Hesser, J. E. 1993, in The Globular Cluster-Galaxy Connection, ed. Smith & Brodie (ASP Conf. Ser. 48), 1
Huebner, W. F., Merts, A. L., Magee, N. H., & Argo, M. F. 1977, Los Alamos Sci. Lab. Rep. LA-6760-M
Hughes, S. M. G., & Wood, P. R. 1990, AJ, 99, 784
Iglesias, C. A., & Rogers, F. J. 1993, ApJ, 412, 752
Iglesias, C. A., Rogers, F. J., & Wilson, B. G. 1992, ApJ, 397, 717
Johnson, H. L. 1966, ARA&A, 4, 193
Johnson, H. R., Ake, T. B., & Ameen, M. M. 1993, ApJ, 402, 667
Kurucz, R. L. 1979, ApJS, 40, 1
———. 1992, in IAU Symp. 149, The Stellar Populations of Galaxies, ed. B. Barbuy & A. Renzini (Dordrecht: Kluwer), 225
Lançon, A., & Rocca-Volmerange, B. 1992, A&AS, 96, 593
Lançon, A., & Wood, P. R. 1995, in preparation
Le Berte, T., Epchtein, N., Guglielmo, F., & Le Sidaner, P. 1994, in Science with Astronomical Near-Infrared Sky Surveys, ed. N. Epchtein, A. Omont, B. Burton, & P. Persi (Dordrecht: Kluwer), 105
Le Borgne, J. F., Pello, R., Rocca-Volmerange, B., Lançon, A., Bruzual A., G., & Sanahuja, B. 1995, in preparation
Lee, Y. W. 1994, ApJ, 423, 248
Leitherer, C., & Heckman, T. M. 1995, ApJS, 96, 9
Lejeune, T. 1995, Ph.D. thesis, Univ. Strasbourg, in preparation
Lequeux, J., Peimbert, M., Rayo, J. F., Serrano, A., & Torres-Peimbert, S. 1979, A&A, 80, 155
Liebert, J., Saffer, R. A., & Green, E. M. 1994, AJ, 107, 1408
Maeder, A. 1975, A&A, 40, 303
Maeder, A., & Conti, P. S. 1994, ARA&A, 32, 227
Magris, G., & Bruzual A., G. 1993, 417, 102
Mayya, Y. D. 1995, AJ, 109, 2503
McWilliam, A., & Rich, R. M. 1994, ApJS, 91, 749
Meyer, M. R., Edwards, S., Hinkle, K., Skrutskie, M. F., & Strom, S. E. 1995, in Disks and Outflows around Young Stars, ed. S. Beckwith (Heidelberg: Springer), in press
Meynet, G., Mermilliod, J. C., & Maeder, A. 1993, A&AS, 98, 477
Ortolani, S., Barbuy, B., & Bica, E. 1990, A&A, 236, 362
Paczyński, B. 1970, Acta Astron., 20, 47
Pagel, B. E. J., Simonson, E. A., Terlevich, R. J., & Edmunds, R. G. 1992, MNRAS, 255, 325
Park, Y. H., & Lee, Y. W. 1995, ApJ, submitted
Peletier, R. F. 1989, Ph.D. thesis, Univ. Groningen
Persson, S. E. 1987, unpublished
Persson, S. E., Aaronson, M., Cohen, J. G., Frogel, J. A., & Mathews, K. 1983, ApJ, 266, 105
Peterson, R. C., Dalle Ore, C. M., & Kurucz, R. L. 1993, ApJ, 404, 333
Reimers, D. 1975, Mem. Soc. Roy. Sci. Liège, 8, 369
Renzini, A. 1994, A&A, 285, L5
Renzini, A., & Fusi Pecci, F. 1988, ARA&A, 26, 199
Renzini, A., & Voli, M. 1981, A&A, 94, 175
Rich, M. R., Mould, J. R., & Graham, J. R. 1993, AJ, 106, 2252
Richer, J., Michaud, G., & Profitt, C. R. 1992, ApJS, 82, 329
Ridgway, S. T., Joyce, R. R., White, N. M., & Wing, R. F. 1980, ApJ, 235, 126
Rogers, F. J., & Iglesias, C. A. 1992, ApJ, 401, 361
Schaller, G., Schaerer, D., Meynet, G., & Maeder, A. 1992, A&AS, 96, 269
Schmutz, W., Leitherer, C., & Gruenwald, R. 1992, PASP, 104, 1164
Schönberner, D. 1983, ApJ, 272, 708
Searle, L., Wilkinson, A., & Bagnuolo, W. G. 1980, ApJ, 239, 803
Seaton, M. J., Yan, Y., Mihalas, D., & Pradhan, A. K. 1994, MNRAS, 266, 805
Straizys, V., & Sviderskiene, Z. 1972, Bull. Vilna. Astron. Obs., 35, 1
Stringfellow, G. S., Bodenheimer, P., Noerdlinger, P. D., & Arigo, R. J. 1983, ApJ, 264, 228
Stryker, L. L. 1993, PASP, 105, 1081
Tantalo, R., Bressan, A., Chiosi, C., & Fagotto, F. 1995, A&A, submitted
Terndrup, D. M., Frogel, J. A., & Withford, A. E. 1991, ApJ, 378, 742
Tinsley, B. M. 1972, ApJ, 178, 319
———. 1978, ApJ, 222, 14
Tripicco, M. J., Dorman, B., & Bell, R. A. 1993, AJ, 106, 618
Tsuji, T. 1978, A&A, 62, 29
———. 1981, A&A, 99, 48
Vacca, W. D. 1994, ApJ, 421, 140
VandenBerg, D. A. 1983, ApJS, 51, 29
———. 1985. ApJS, 58, 711
VandenBerg, D. A., & Bell, R. A. 1985, ApJS, 58, 561
VandenBerg, D. A., & Laskarides, P. G. 1987, ApJS, 64, 103
van den Bergh, S. 1981, A&AS, 46, 79
Vassiliadis, E., & Wood, P. R. 1993, ApJ, 413, 641
Vauclair, S., & Charbonnel, C. 1995, A&A, 295, 715
Weidemann, V. 1987, A&A, 188, 74
Weiss, A., Peletier, R. F., & Matteucci, F. 1995, A&A, 296, 73
Wood, P. R.1994, in Science with Astronomical Near-Infrared Sky Surveys, ed. N. Epchtein et al. (Dordrecht: Kluwer), 121
Worthey, G. 1994, ApJS, 95, 107 (GW)
Worthey, G., Gaber, S. M., & González, J. J. 1992, ApJ, 398, 69
Worthey, G., Faber, S. M., González, J. J., & Burstein, D. 1994, ApJS, 94, 687
Worthey, G., Trager, S. C., & Faber, S. M. 1995, in Fresh Views on Elliptical Galaxies, ed. A. Buzzoni, A. Renzini, & Serrano (ASP Conf. Ser.), in press
Zijlstra, A. A., Loup, C., Waters, L. B. F. M., & de Jong, T. 1992, A&A, 265, L5